R-7995

INTERIM REPORT,

CORRELATION OF SPRAY DROPSIZE DISTRIBUTION AND INJECTOR VARIABLES

by

R. M. Knight
W. H. Nurick

prepared for

NATIONAL AERONAUTICS AND SPACE ADMINISTRATION

Contract NAS7-726

ROCKETDYNE
A DIVISION OF NORTH AMERICAN ROCKWELL CORPORATION
6633 CANOGA AVENUE, CANOGA PARK, CALIFORNIA 91304

R-7995

INTERIM REPORT

CORRELATION OF SPRAY DROPSIZE DISTRIBUTION AND INJECTOR VARIABLES

by

R. M. Knight
W. H. Nurick

prepared for

NATIONAL AERONAUTICS AND SPACE ADMINISTRATION

30 September 1969

Contract NAS7-776

Rocketdyne
A Division of North American Rockwell Corporation
6633 Canoga Avenue, Canoga Park, California

FOREWORD

This report was prepared for NASA, Jet Propulsion Laboratory, Pasadena, California, by Rocketdyne, a Division of North American Rockwell Corporation. The study was conducted in accordance with Contract NAS7-726, G.O. 09162.

Mr. R. M. Clayton of the Jet Propulsion Laboratory served as NASA Technical Project Manager. The Rocketdyne Program Manager was Mr. T. A. Coultas. Technical approach and guidance of the program was directed by Mr. S. D. Clapp, who functioned as Project Manager.

ABSTRACT

A 7-month applied research program was conducted to determine the effects of liquid miscibility and several injector design variables on spray dropsize and size distribution. The method of frozen wax was used throughout the program to provide a quantitative measure of these effects. In the miscibility studies, experiments were conducted with unlike-doublet elements of varying diameter ratio to ascertain the effects of miscibility on droplet size and distribution. In addition, investigations were conducted with unlike-doublet and pentad elements to determine the level of emulsification which occurs when two immiscible liquid jets impinge.

In the investigation of injector design variables, single-element injectors of like-doublet, unlike-doublet, and pentad configurations were flowed at low injection velocities (30 to 60 ft/sec) to extend previous dropsize correlations to the low velocity regime. Experiments were also conducted with a co-planer triplet element over a velocity range of 30 to 170 ft/sec. In addition, wax flow experiments were made at several impingement angles and free jet length-diameter ratios using a like-doublet element configuration.

CONTENTS

ILLUSTRATIONS

TABLES

INTRODUCTION

The evaluation of rocket engine injector design criteria requires an understanding of the primary injection parameters which control the combustion process. Previous analytical and experimental work by Rocketdyne and other investigators had shown that combustion in liquid rocket engines is limited in rate by the vaporization of the liquid propellants, a process which is primarily dependent upon spray droplet size and propellant physical properties. Dropsize is, therefore, an important parameter in the determination of rocket engine combustion efficiency.

Attempts to predict droplet size distributions theoretically have, for the most part, been unsuccessful. The first theoretical contribution to this field was given by Rayleigh (Ref. 1) in his analysis of the instabilities associated with a single jet of liquid. Many other workers have extended the works of Rayleigh (e.g., Ref. 2 through 6); however, they have been unable to predict, to an adequate degree, the character of these spray droplet size distributions.

Complicating any theoretical predictions of droplet size distributions is the existence of different flow regimes in which spray formation processes are controlled by different effects. At low injection velocites, surface tension forces predominate in the liquid breakup processes. At higher injection velocities, aerodynamic shear forces between the liquid and the gaseous environment become important. At very high injection velocities, the liquid is exposed to rapid deceleration by the gaseous environment, and inertial forces thus become important. Some of these flow regimes have been observed experimentally (e.g., Ref. 6 through 9), and theoretical considerations of the existence of the different regimes have been recorded in the literature (Ref. 2 and 3). Because of the difficulties involved in the theoretical prediction of spray droplet sizes, many investigators have determined spray droplet sizes experimentally for various atomizer configurations and liquid physical properties (e.g., Ref. 10 through 13). However, the data reported by these investigators in the

literature are primarily for injector types and operating conditions which are not comparable to those found in typical rocket engines. Notable exceptions to this are the works of Dombrowski and Hooper (Ref. 12), Ingebo (Ref. 13), and a recent study at Rocketdyne (Ref. 14).

Dombrowski and Hooper conducted a study of the factors influencing the disintegration of sheets formed by the impingement of two water jets. The investigation was limited to like-doublet elements having an orifice L/D of 400. Impingement angle was varied and a dropsize correlation was developed. The work of Ingebo included effects of orifice diameter, jet velocity, and velocity difference between the liquid jet and a surrounding airstream. This investigation utilized short orifice elements ($L/D \approx 10$) and n-heptane as the propellant simulant. In both studies, a photographic method was used for measurement of the spray particle sizes. This technique has limitations because the results are generally dependent upon the size and location of the photographic field. In addition, reduction of data from the spray photographs is time consuming and costly.

The most recent study at Rocketdyne (Ref. 14) had shown that the molten wax technique could be successfully utilized to provide a quantitative measure of the sprays produced by impinging stream injector elements. This experimental method has advantages in that the entire spray field is collected and particle sizes are determined using a simple sieve analysis.

The previous Rocketdyne study was also instrumental in extending previous atomization work in the areas of rocket engine injector simulation. It was demonstrated that two immiscible liquids (water and paraffin wax) could be used for simulation of unlike impinging injector elements. In addition, it was shown that the propellant atomization and mixing processes could be investigated separately and the results combined to determine an overall predicted combustion efficiency.

Although the Ref. 14 program added significantly to a better understanding of injector atomization, many areas of interest required investigation. For

example, one area which had not been thoroughly studied included the effects of impinging two immiscible jets on dropsize and size distribution and the possibility of forming an emulsion.

In the realm of orifice geometry and injector design effects on dropsize, only limited work has been done. Various orifice length-diameter ratio jets have been utilized; however, the effects of this important parameter had not been studied specifically. In addition, little or no information was available in the areas of free jet geometry and low injection velocity operation. The overall goals of the current study were to fill these gaps and provide a more basic understanding of the atomization characteristics of rocket engine injectors.

SUMMARY

The purpose of this study was to experimentally investigate poorly understood aspects of the mechanism of atomization and to extend the range of previous dropsize correlations. The results of this program have been instrumental in providing a more basic understanding of the parameters which significantly influence the atomization process. The effects of many of these parameters were not individually determined; however, the results have defined specific areas of interest which warrant further investigation.

A summary of the pertinent observations regarding the experimental study are as follows:

1. During the propellant miscibility studies, it was found that, within the limits of experimental accuracy, the mass median dropsize is the same for both miscible and immiscible impingement.
2. Miscibility did effect, to a small extent, the dropsize distribution. In all cases, the size distribution resulting from immiscible impingement was closer to the monodisperse than that for the corresponding miscible impingement.
3. Diameter ratio was also found to influence dropsize and size distribution of unlike doublet injectors. At equal injection velocities, the smaller of the two jets will yield the smaller dropsize and a more nearly monodisperse distribution.
4. For an unlike doublet element incorporating a 1.36 diameter ratio (d_{ox}/d_f), it was found that, at low stream momentum levels, the fuel dropsize approached a minimum at a specific operating condition. The diameter ratio was not sufficiently large, however, to determine whether the mixing parameter or dynamic pressure ratio was the relevant variable.

5. The results of the emulsification studies showed that the magnitude of the emulsion is about 1 percent over a wide range of total stream momentum for both unlike doublet and pentad injectors. From the standpoint of rocket engine performance correlation, the 1-percent emsulsion level is not considered large enough to detract from the presently used assumptions of discrete fuel and oxidizer sprays.

6. The low injection velocity studies showed that dropsize dependence on injection velocity is considerably different at low and high velocities. Various reasons for this behavior are postulated: (1) variations in the upstream flow conditions, (2) a change in the dominant mechanisms which control droplet breakup, and (3) secondary atomization effects resulting from flowing the elements in a stagnant atmosphere.

7. It was also found that free jet impingement length can produce significant changes in the droplet size produced by like-doublet elements. Stream turbulence and velocity profile, jet disintegration, and misalignment are postulated as the dominant variables which influenced droplet breakup.

APPARATUS

SINGLE-ELEMENT INJECTORS

Two of the objectives of this program include the attainment of high quality, reproducible dropsize data, and the comparison of dropsizes produced by injectors having different hydraulic flow control characteristics. To achieve this first objective, single-element injectors incorporating a long orifice length and a contoured entrance were used in the majority of the wax flow experiments. Orifices designed with a 50:1 L/D and a rounded inlet have been found by Rupe (Ref. 15) to produce free jets that are stable, symmetrical, and reproducible. The second objective was fulfilled by conducting flows under similar conditions with relatively short (10:1 L/D) injector elements. The 10:1 elements, which were used in the low injection velocity studies in Task IIA, were available from a previous Rocketdyne program.

The program requirements of various injector types (like-doublet, unlike-doublet, pentad, and triplet), and variations of impingement angle and free jet length (like-doublet only) suggested the desirability of an adjustable injector to minimize fabrication costs. A single-element injector was designed and fabricated to incorporate the 50:1 L/D elements which are described in the following section.

A schematic of this injector is shown in Fig. 1. The basic assembly consisted of a base plate, tube clamps, tube holders, and the long L/D orifices. With these components, various combinations of like-doublet, unlike-doublet, and coplaner triplet elements could be assembled. Adjustment features of this assembly included variations of included impingement angle from 45 to 90 degrees, free jet length from 1 to 10, and orifice diameter from 0.063 to 0.128 inch. The pentad (4-on-1) configuration required the addition of two side plates, and the associated clamps, posts and orifices. Adjustment features of the pentad element were the same as those listed above.

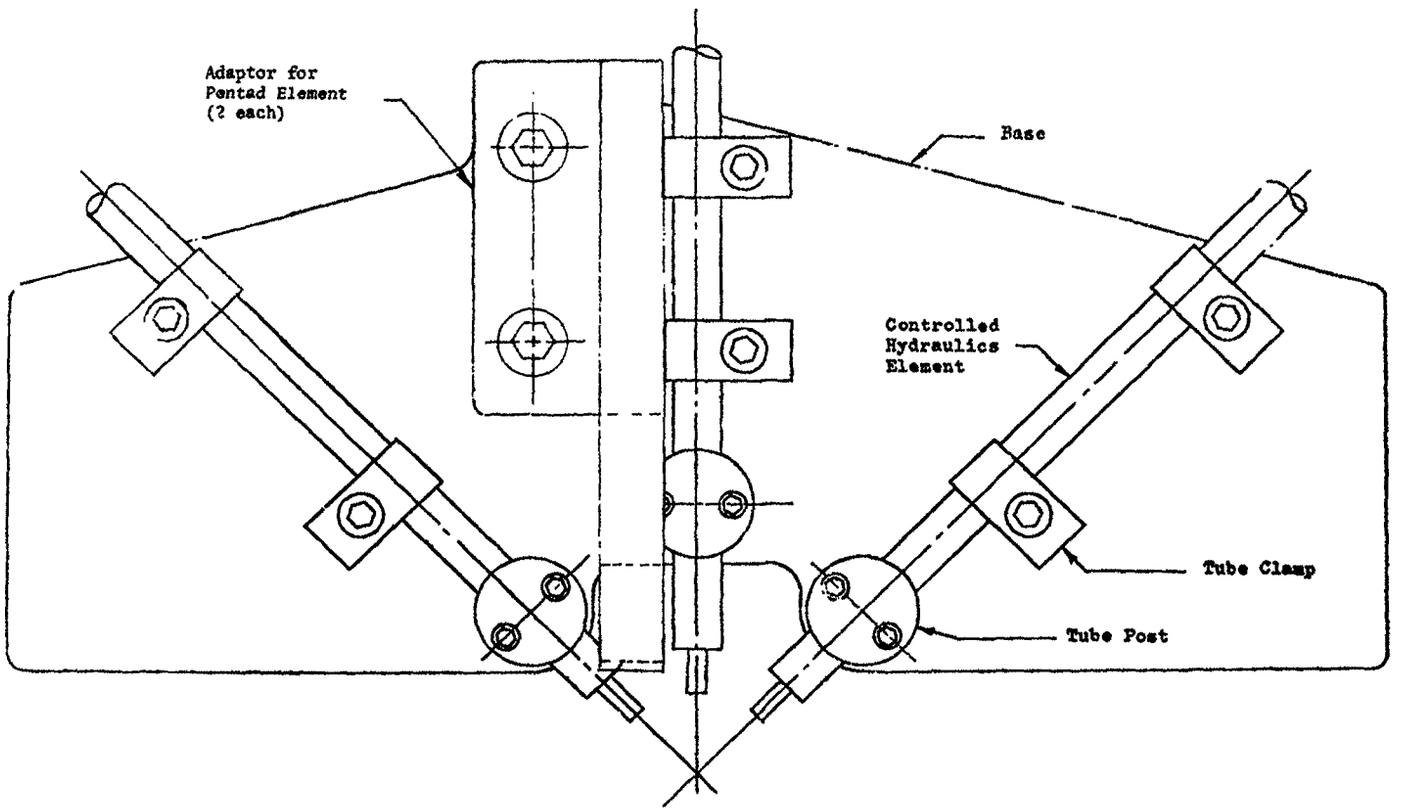

Figure 1. Adjustable Injector Design Incorporating Controlled Hydraulics (L/D = 50) Elements (Triplet Configuration Shown)

Photographs of the injector assembly are illustrated in Fig. 2. A pentad element having a free jet length of 5 and an impingement angle of 60 degrees is shown. All components were constructed of aluminum.

Long (50:1) L/D Elements

The first consideration in the design of the 50:1 L/D orifices was the method of fabrication. Several techniques were considered, including drilling and reaming, electrical discharge machining, and the use of tubing. The latter method was chosen on the basis of both quality control and economy. In addition, the use of tubular elements permitted the fabrication of an adjustable injector in which various element types could be constructed.

Typical geometry of the controlled hydraulics orifices is shown in Fig. 3. The orifices were constructed from three aluminum tubes, with the outer tubes swaged over the inner tube which comprised the 50:1 L/D orifice. The inner tubes were initially 0.004 to 0.008 inch undersize and then reamed to the final diameter after the swaging process. A total of 10 orifices were constructed, six with a diameter of 0.063-inch, and two each with diameters of 0.086 and 0.128 inch.

The 10 orifices were calibrated over a range of 25 to 300 psi ΔP with water. The purpose of this was twofold: (1) to provide matched sets of orifices for the like doublet, triplet, and pentad configurations, and (2) to visually inspect the flow and impingement quality. Measured discharge coefficients were 0.73 ±0.02 for each of the orifices. Motion pictures of the free jets and impinging doublets were taken at mean jet velocities of 50 and 100 ft/sec. Superficially, the jets appeared similar to those of Ref. 15 for fully developed turbulent flow at the same mean jet velocities.

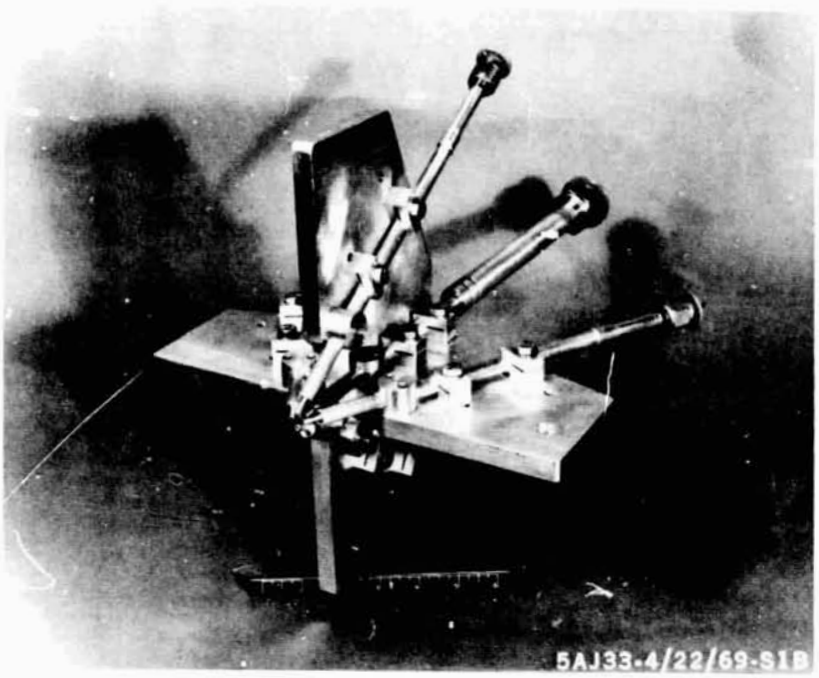

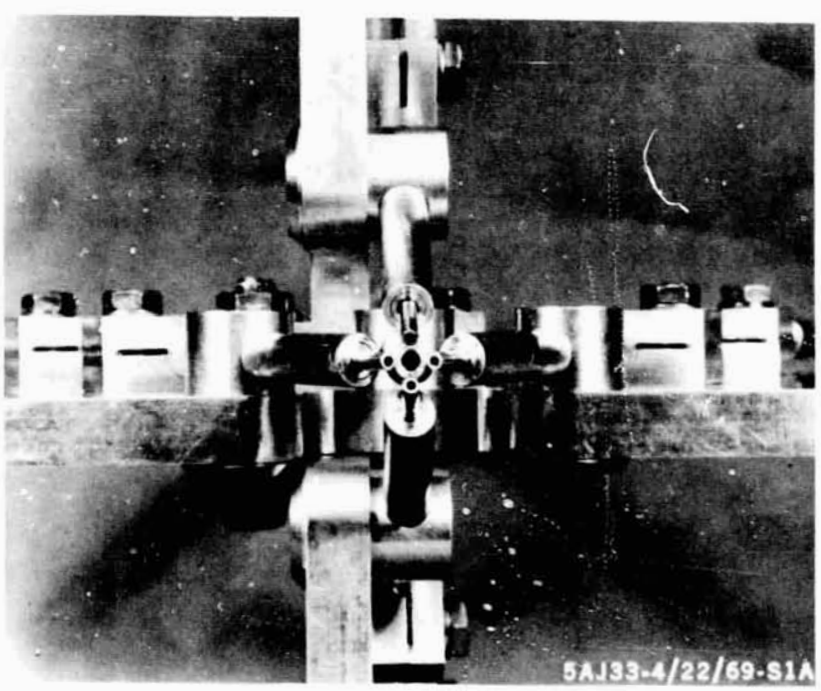

Figure 2. Adjustable Tube Injector Incorporating Controlled Hydraulics Orifices (Pentad Element Shown)

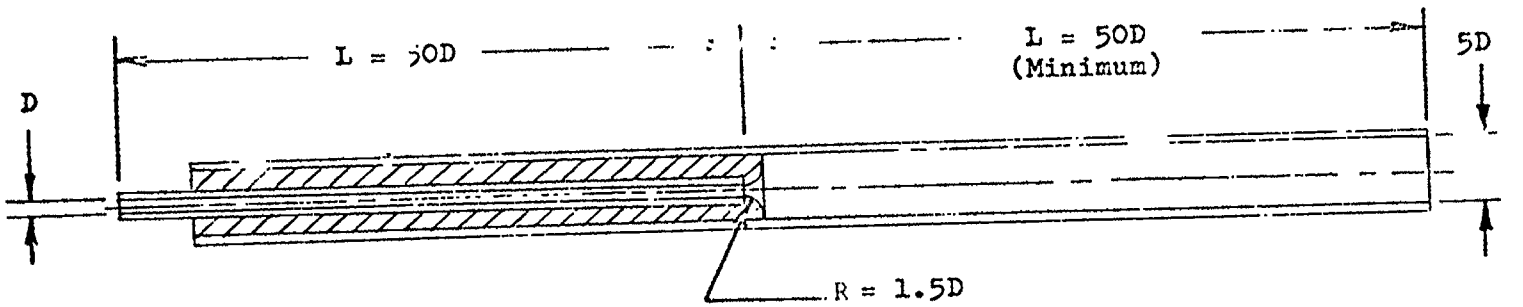

Figure 3. Typical Orifice Geometry for Controlled Hydraulics Injector

Short (10:1) L/D Elements

The 10:1 L/D orifices used in the low injection velocity studies of Task IIA are shown schematically in Fig. 4. A total of five elements were used; two like-doublets, two unlike-doublets and one pentad. The orifice geometry for each element is summarized in Table 1.

TABLE 1

ORIFICE GEOMETRY FOR 10:1 L/D ELEMENTS,
NOMINAL FREE JET LENGTH = 5 DIAMETERS

Element Type	Fuel Orifice Diameter, inch	Oxidizer Orifice Diameter, inch	Upstream Feed or Tube Diameter, inch
Like-Doublet	0.063	--	0.180
Like-Doublet	0.081	--	0.250
Unlike-Doublet	0.063	0.086	0.180/0.250
Unlike-Doublet	0.063	0.128	0.180/0.370
Pentad (Four Oxidizers Impinging on Central Fuel)	0.086	0.063	0.250/Integral Manifold

NOTE: For $D_f \neq D_{ox}$. the nominal free jet length is based upon the average diameter

For the like- and unlike-doublet elements, the entrance geometry consisted of a straight tube having a cross section of three orifice diameters and a length of approximately 17 diameters. This entry length-to-diameter ratio is relatively short in that it does not permit the establishment of fully developed flow (either laminar or turbulent) at the orifice entrance. Combined with the relatively short orifice length of 10 jet diameters, the orifice flow at the exit is therefore not independent of the entry flow. This is in contrast to the long (50:1) L/D orifice, where the orifice length is sufficient for the establishment of fully developed flow.

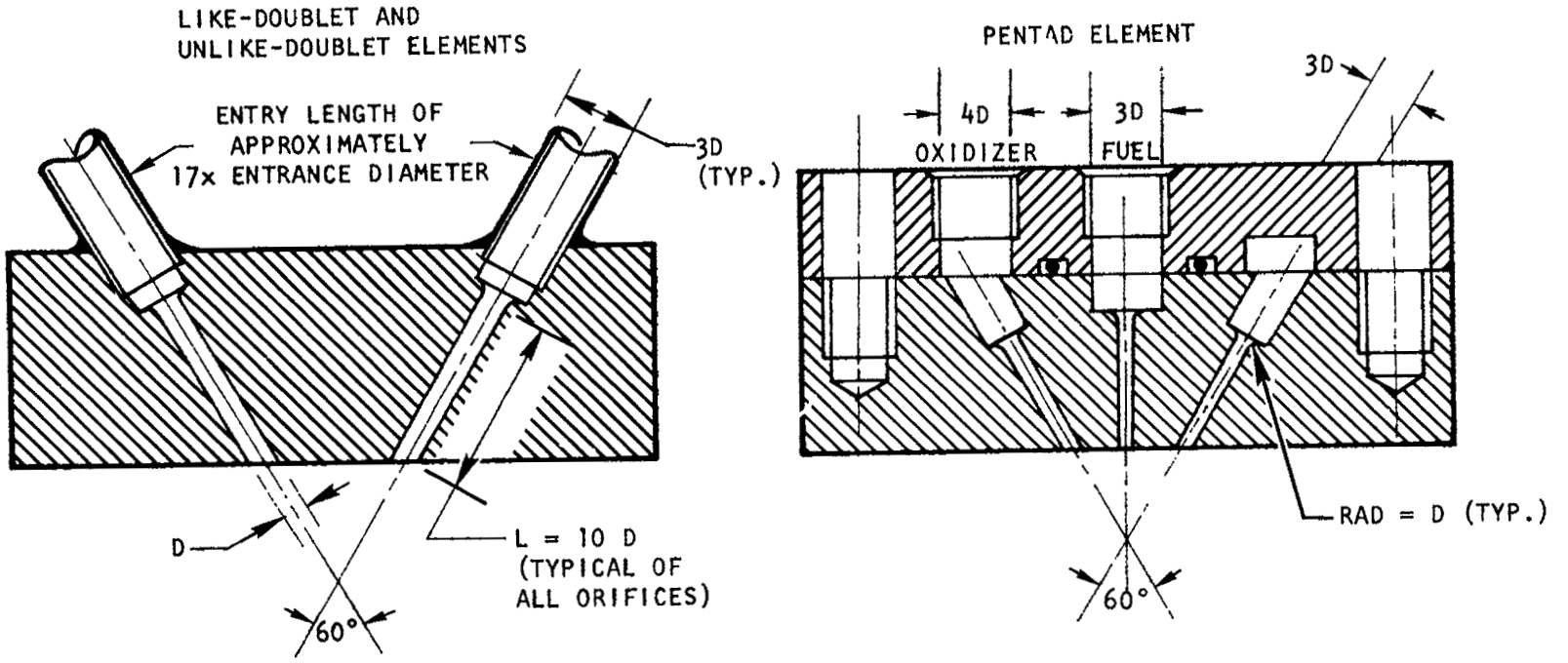

Figure 4. Schematics of Short (10:1) L/D Elements Used in Low Injection Velocity Studies

The inlet geometry for the pentad element was somewhat different as shown in Fig. 4. The outer four orifices (oxidizer) were fed from an annular manifold. The central fuel orifice was fed from a straight tube having a cross section of three jet diameters and a length of approximately 17x the entrance diameter.

It should be noted that all of the 10:1 L/D elements used in Task II were identical to those of the Ref. 14 program. All comparisons of present and previous short orifice data are made on the basis of similar entrance and orifice geometry.

Propellant Simulants

Three propellant simulants were used during this study: Shell Type 270 paraffin wax, water, and a solution consisting of 75-percent (by volume) diethanolamine and 25-percent water. A summary of the pertinent physical properties at the nominal injection temperature of 200 F is given below:

	Density, lb/ft^3	Viscosity, lbm/ft-sec	Surface Tension, dynes/cm
Shell 270 Wax	47.7	2.02×10^{-3}	25
Water	60.1	2.05×10^{-4}	60
75% DEA-25% H_2O	63.9	2.0×10^{-3}	NA

WAX FLOW FACILITY

The wax flow facility used for the dropsize measurements is shown in Fig. 5a and 5b. The overall system consisted of wax and water supply tanks immersed in a hot oil bath container and a particle collector which catches the frozen wax particles. Instrumentation used to measure pressure, flowrate and temperature consisted of strain gauge transducers, turbine flowmeters and iron-constantan thermocouples, respectively.

Each wax and water tank had an independent pressurizing and vent system. Also, as illustrated in Fig. 6 and 7, each product out line had three flowmeters, thermocouples, and hand shutoff valves arranged in parallel so a wide range of flowrates could be obtained. The hot oil bath, shown schematically in Fig. 8, was heated by means of a 30 kilowatt, thermostatically controlled heater. An electrically operated pump circulated the oil from the oil bath container through the heater and back. Also, hot oil was forced through jacketed run lines and valves to ensure that the wax did not freeze in the feed lines.

The particle collector, shown in Fig. 5b, is a 18 by 50 foot epoxy-coated wooden platform which is located under a roofed structure. The injector end of the collector is surrounded by a large canvas (not shown in the figure) to reduce wind currents which would cause the smaller particles to be blown away.

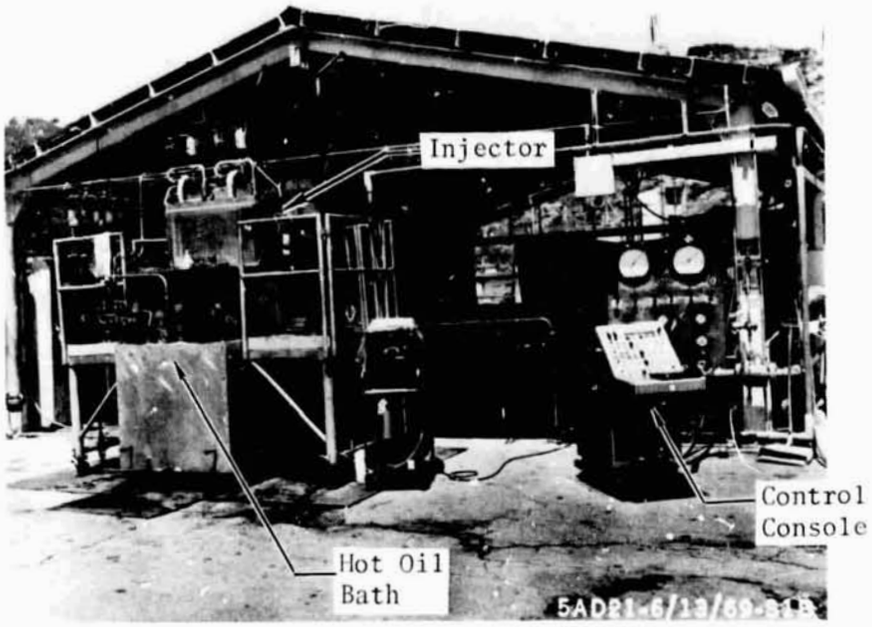

a. Wax Flow System

b. Particle Collector

Figure 5. Wax Flow Facility

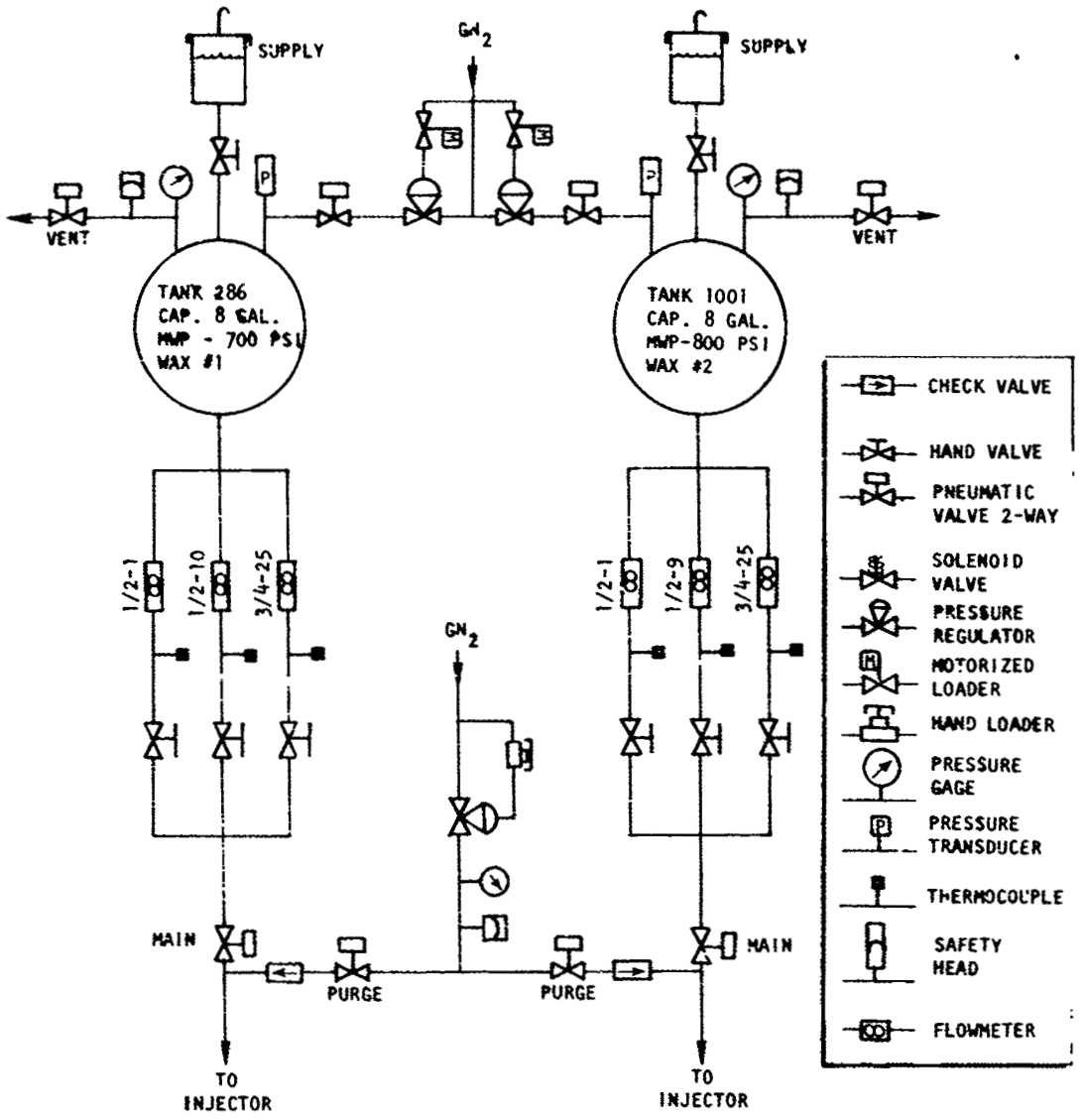

Figure 6. Schematic of Hot Wax System

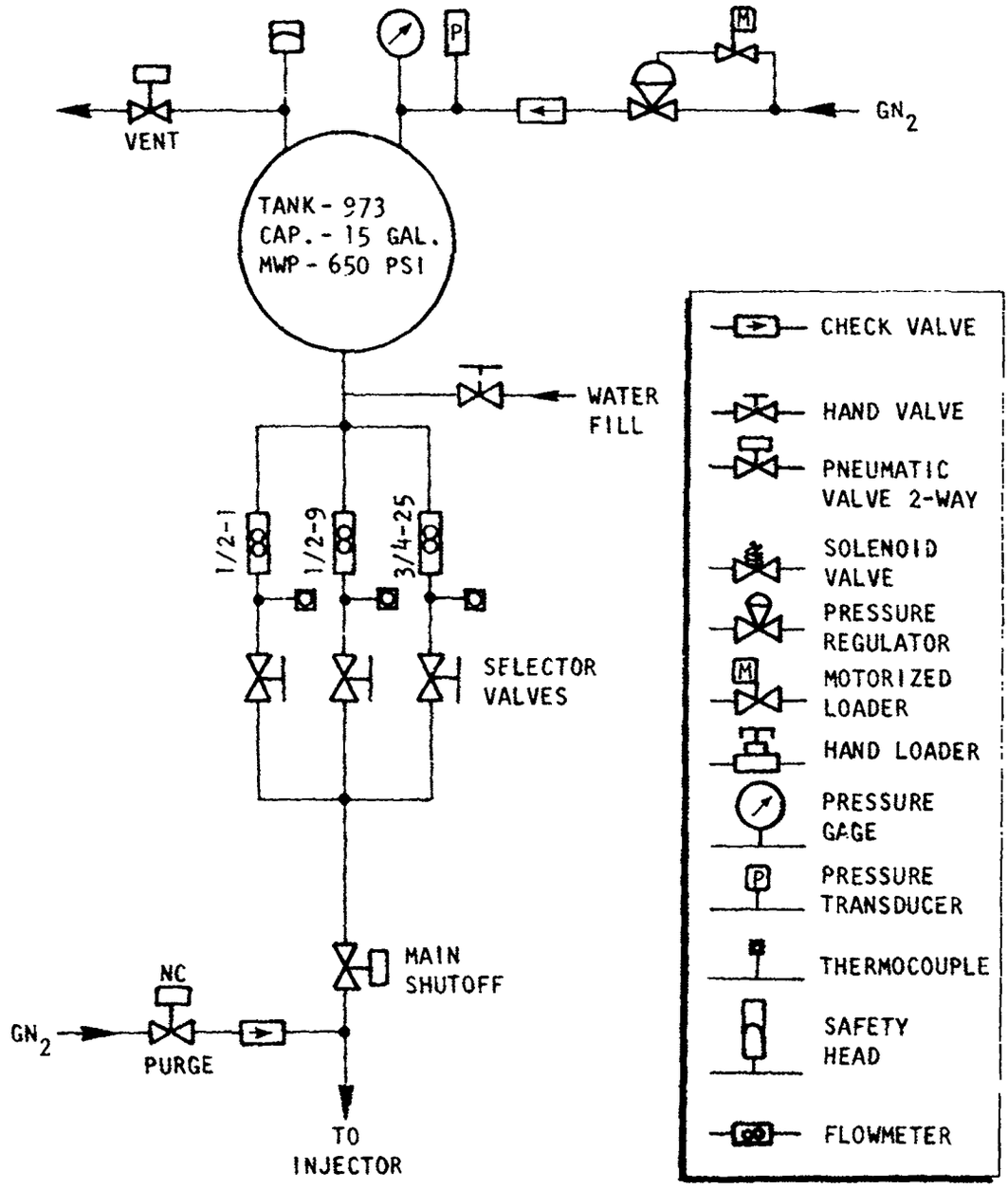

Figure 7. Schematic of Hot Water System

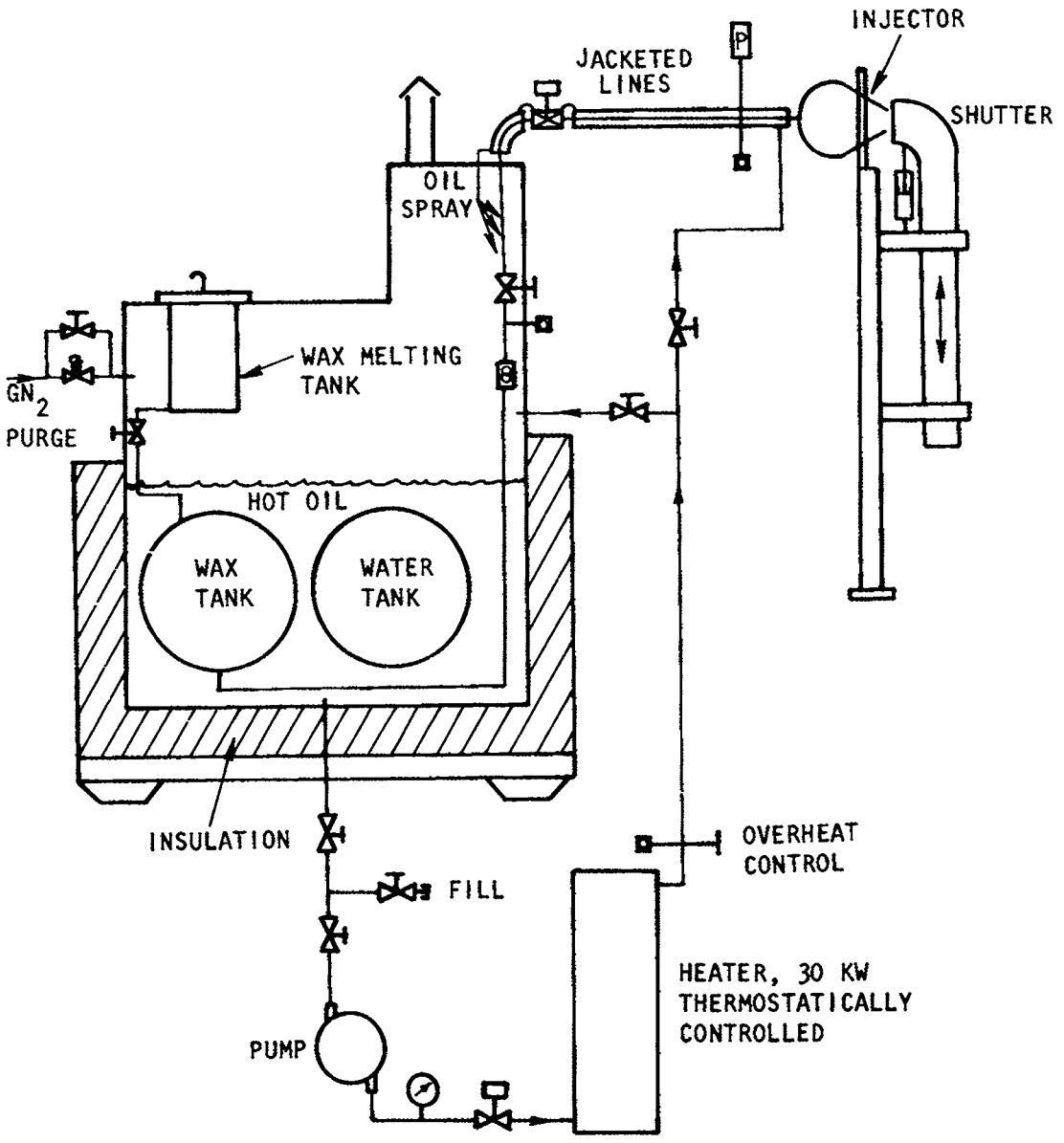

Figure 8. Schematic of the Hot Oil System

PROCEDURES

WAX SPRAY PROCEDURE

The experimental procedure for droplet size measurement was as follows:

1. The injector configuration was installed on the wax facility so that the wax spray created by the orifices after freezing during its ballistic trajectory strikes the particle collector.
2. The electrical oil heater and pump were turned on to bring the propellant simulant tanks and run lines up to 210°F.
3. After all parts of the system were heated and instrumentation requirements checked, the run tanks were heated and the run tanks were pressurized.
4. With the piston operated shutter in the up position, the test was initiated by actuating the main pneumatic shutoff valves. When the flowrates and injection pressures reached a steady condition, the shutter was actuated and the wax particles were allowed to spray onto the particle collector. The use of the shutter minimized the influence of start and stop transients on the size distribution of the collected particles.
5. The injector flow was continued for approximately 10 seconds. The shutter was then actuated to the up position and main shut-off valves closed.
6. The tanks were then vented and systems secured.
7. The particles were washed from the collector into the catch basin, where they were scooped from the surface of the water and placed in a plastic bag for temporary storage.

PARTICLE SAMPLE ANALYSIS

The following procedure was used for the analysis of the particles:

1. A 100-gram sample of wax particles was placed in a Buchner funnel and subjected to suction for removal of water.

2. After the particles had been partly dried by suction, they were placed on a large tray in a vacuum chamber for a period of at least 48 hours to ensure that the particles were completely dry.

3. After drying, a random 10-gram sample was selected to be sieved. A series of 23 standard testing sieves ranging in size from 53 to 2380 microns was used. For any particular sample, only 12 of the sieves were used; the particular sieve sizes used depended upon the anticipated size range of the particle sample. The sieves were shaken on a "RO-TAP" automatic sieve shaker for 30 minutes, during which time the shaking was stopped every 6 minutes and each sieve struck sharply several times to help release any particles which had become wedged in the sieve screens.

4. After the sieving operation was completed, the mass of particles retained on each sieve was weighed on an electric balance. It was found that with considerable care in transferring the wax from the sieves into the weighing pan, a total recovery of 97 to 99 percent of the mass originally introduced into the sieves was possible. The photographs shown in Fig. 9 are typical of the uniformity of sizes of the solid wax particles obtained by the sieving operation.

5. These data were then converted into the total fraction of mass having a particle size smaller than each of the sieve sizes. An example of the raw data and converted data is shown in Table 2. The data shown in Table 2 are also shown plotted in Fig. 10.

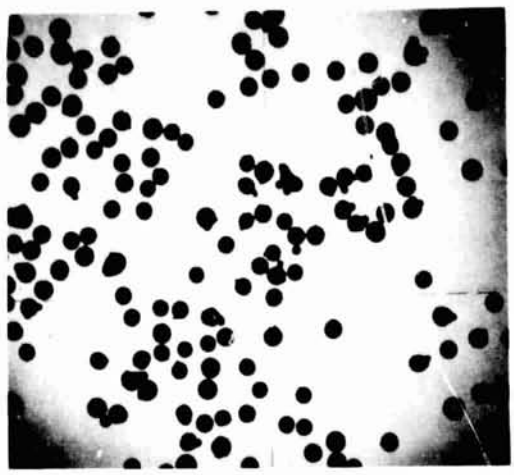

500 Microns

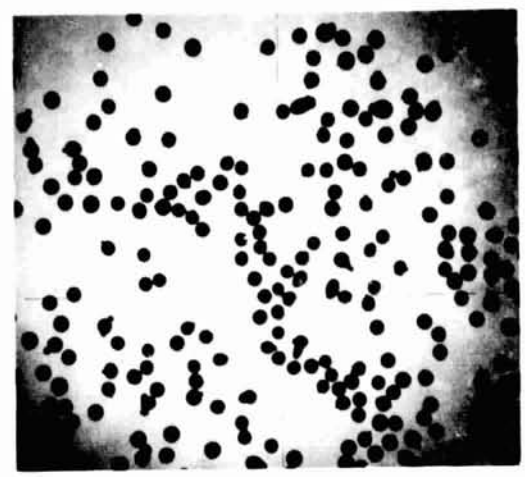

420 Microns

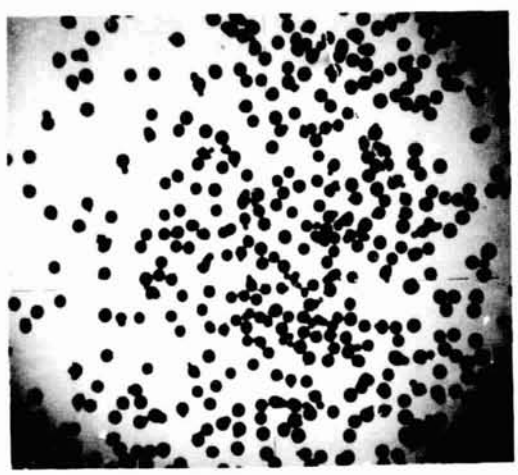

354 Microns

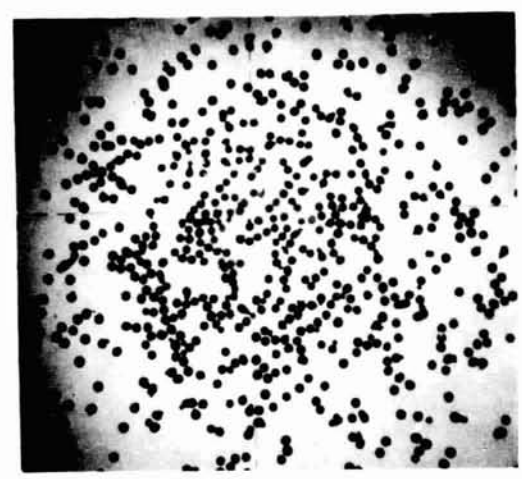

250 Microns

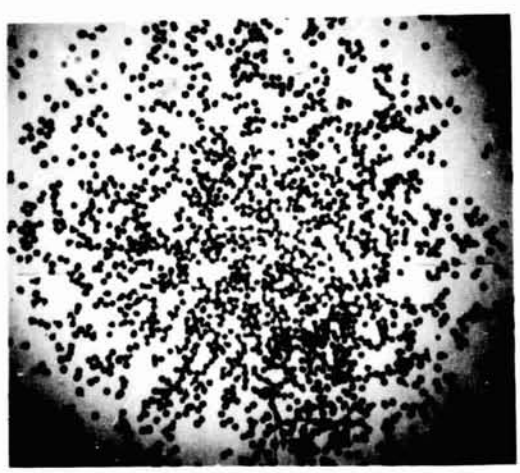

177 Microns

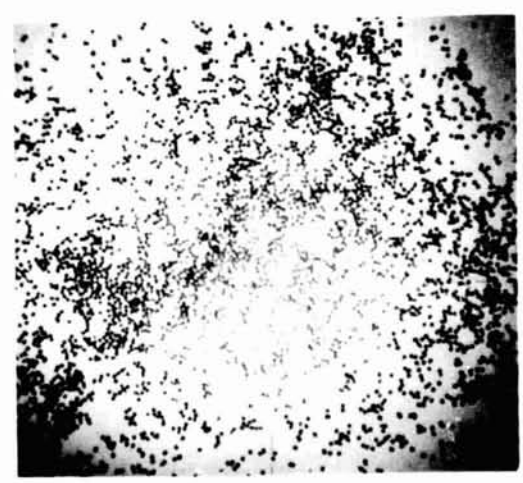

125 Microns

Figure 9. Photographs of Solidified Wax Droplets Using a 0.063-Inch-Diameter Like-Doublet Element

TABLE 2

TYPICAL RESULTS FROM SIEVING ANALYSIS*

Sieve Size, microns	Mass in Sieve, grams	Fraction of Total Mass	Cumulative Fraction of Total Mass Having Particle Size Smaller Than Sieve Size
Catch Pan	0.156	0.0153	--
88	0.139	0.0141	0.0153
105	0.169	0.0170	0.0293
125	0.208	0.0211	0.0464
149	0.667	0.0674	0.0674
177	0.591	0.0598	0.1348
210	1.042	0.1053	0.1946
250	1.201	0.1214	0.2999
297	1.490	0.1507	0.4212
354	1.609	0.1627	0.5719
420	1.138	0.1150	0.7346
500	1.155	0.1168	0.8496
590	0.332	0.0336	0.9664

*0.063-inch-diameter like-doublet injector with free jet length of 5 diameters and ΔP = 100 psi.

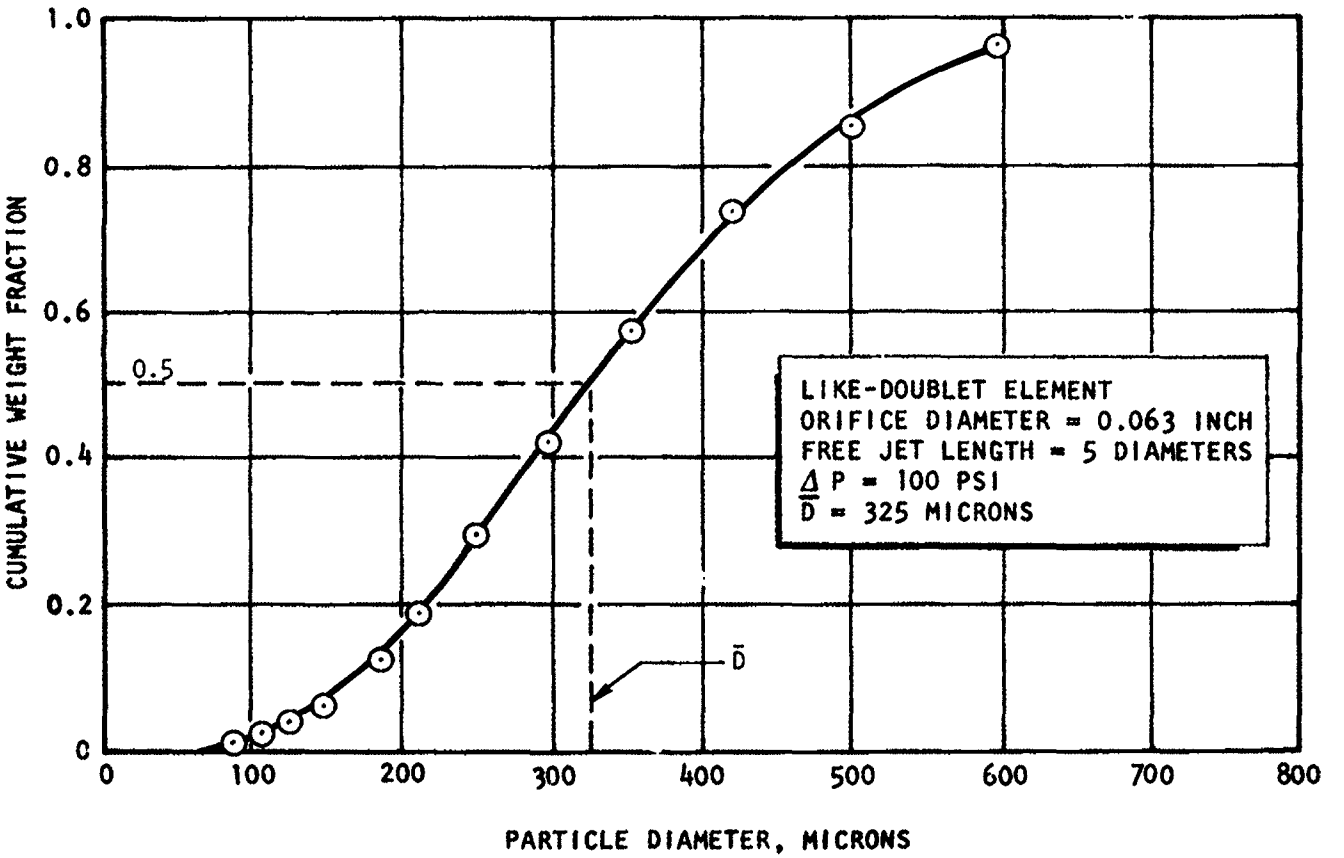

Figure 10. Typical Particle Size Distribution Data Obtained Using the Frozen Wax Technique

DETERMINATION OF DIETHANOLAMINE ENTRAPPED IN WAX DROPLETS

The method developed for the determination of diethanolamine (DEA) entrapped in the wax droplets involved three phases:

1. Removal of the surface DEA
2. Extraction of the entrapped DEA
3. Analysis of the extract solution for DEA

The removal of the surface DEA required repeated washing of the droplet samples using room temperature distilled water in a large extraction funnel. A gas chromatographic analysis for residual DEA was performed after each wash until complete removal was verified. Minimal rinse volumes were used to preclude dilution below analytical detection limits. Experiments were also conducted to verify that DEA was not soluble in the paraffin wax. These experiments included long-term (12 days) surface contact with preformed wax droplets at room temperature to indicate surface uptake and possible solubility. The 12-day soak period revealed no entrapped DEA.

Extractions of the entrapped DEA were performed on a weighed portion of the wax droplets at a temperature such that the wax was molten. The sample was placed in an Erlenmeyer flask on a hotplate and the solution agitated to ensure thorough mixing. This arrangement permitted repeated aqueous extractions of the molten wax. Each portion of the aqueous extract was placed in a volumetric flask for dilution to a known total volume. Precipitates had been observed with low-level DEA solutions during the preparations for the calibrations. The addition of several drops of ammonium hydroxide precluded acidic-carbonate interference and ensured the free base was in solution.

Analysis of the aqueous extract for DEA was accomplished by gas chromatography as follows:

Instrument:	Aerograph 600-D with flame ionization detector
Column:	5 percent DC550 on 40/60 Fluoropak-80, 10 foot by 1/8 inch

Temperatures: Column = 150 C isothermal, injection port = 180 C

Flowrates: Carrier N_2 = 25 ml/min; H_2 = 25 ml/min, Air - 250 ml/min

Readout: Sargent SR recorder, 0 to 1 mv, with Disc Integrator

The absence of chromatographically detectable substances was verified by examinations of aqueous extractions of the bulk wax and droplets formed by wax-wax injector impingement. Positive identification of DEA response using these stated parameters was continuously verified by injection of DEA standards in the range of 0.2 to 1.0 weight percent.

Calibrations were performed using 2- 2- (2- ethoxy ethoxy) ethoxy ethanol as an empirically derived internal standard. The addition of a known concentration of this standard to the prepared DEA/H_2O calibration mixtures yielded a linear nomograph (see Fig. 11), which was independent of minor instrumental and injected sample size differences. The standard was similarly added to the extraction samples, approximating the calibration concentrations.

The selection of 2- 2- (2- ethoxy ethoxy) ethoxy ethanol as an internal standard was made to meet the criteria established by the chromatographic parameters required for DEA detection. Lower homologs of this compound had been used successfully under these same conditions, demonstrating symmetrical peaks and reproducible retention times. The ethoxy ethanols are typically water soluble and have demonstrated both chemical and thermal stability under these chromatographic conditions. The addition of each ethoxy group to the parent ethanol increases the molecular weight which allows predictable retention times in relationship to DEA.

Sample Calculation

Chromatogram. A typical analysis chromatogram with peaks for DEA and the internal standard is shown in Fig. 12. Note the absence of a water peak even though the sample was an aqueous extract. This is because of the fact that the flame ionization detector responds only to carbon containing organic compounds.

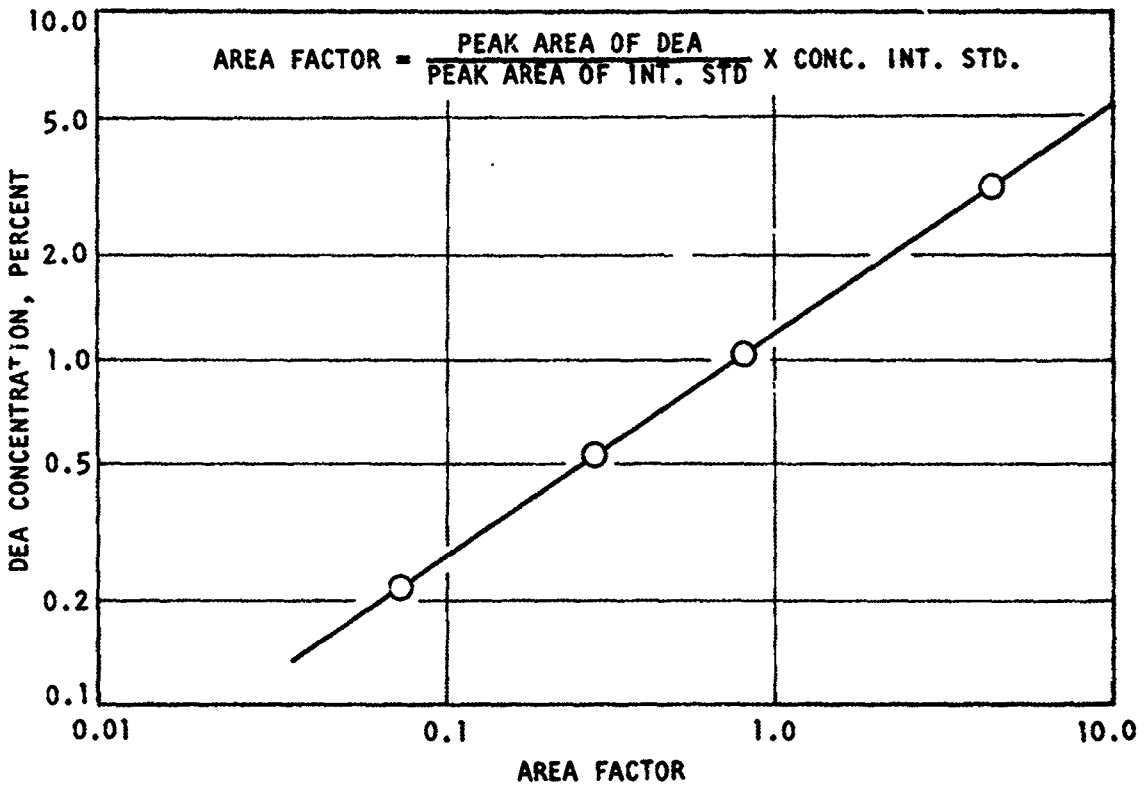

Figure 11. Diethanolamine Calibration Using an Internal Standard

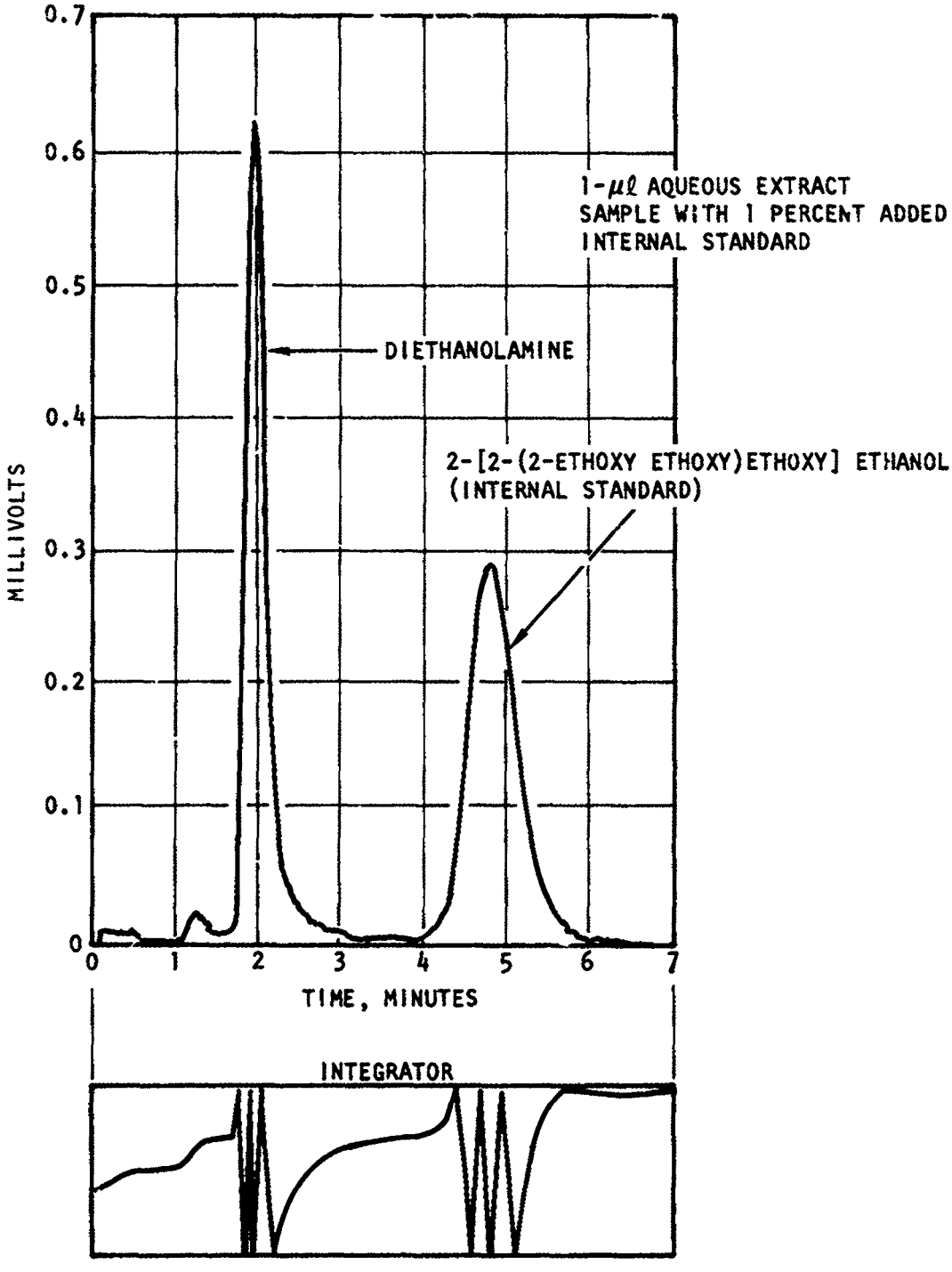

Figure 12. Diethanolamine Analysis Chromatogram

Calculations. The entrapped DEA in wax concentration was calculated from the known wax sample weight, the total extraction volume, and the concentration of DEA in the extract. A stepwise sample calculation is presented below.

1. Weight of dry wax sample (surface DEA removed), grams = 38.96
2. Total Volume of Extract, milliliter = 30.0
3. Concentration of Internal Standard, percent = 0.728
4. From sample chromatogram, $\frac{\text{Peak Area of DEA}}{\text{Peak Area of Int. Std.}}$ = 1.06
5. Area Factor = $\frac{\text{Peak Area of DEA x Concentration of Internal Standard}}{\text{Peak Area of Internal Standard}}$
6. From the nomograph (Fig. 11),

   Area Factor 0.772 = 1.0% DEA in the 30.0-ml extract which weighed 30 grams
7. Concentration of DEA in Wax Sample = $\frac{\text{(1\% DEA) (Weight of extract)}}{\text{Weight of Original Sample}}$

   Concentration of DEA in Wax Sample = $\frac{(1.0\%)\ (30.0\ \text{gm})}{38.96\ \text{gm}}$ = 0.8%
8. Concentration of DEW* in Wax sample = % DEA/0.75

   Concentration of DEW in Wax sample = $\frac{0.8}{0.75}$ = 1.07%

*DEW denotes the DEA-H_2O solution.

RESULTS AND DISCUSSION

The experimental technique used to determine droplet size and dropsize distribution was the method of frozen wax. The experimental approach was designed to determine variations in droplet size and droplet size distribution with changes in specific injector geometric and hydraulic parameters. The ability to distinguish between measured variations in the atomization characteristics is determined by the accuracy and repeatability of the experiment. Consequently, prior to the presentation of the experimental results for each of the four program tasks some aspects of the data quality are discussed.

Because of its desirable sieving characteristics, Shell type 270 wax was selected for use as the propellant simulant. Utilizing the Shell 270 molten wax can present some problems in data reduction. Specifically, when the wax droplets freeze, they first form a solid outer shell which remains rigid. When further freezing of the remaining core takes place, a hollow core is formed because the wax specific gravity changes from 0.79 to 0.92. Visual observation of the droplets under a microscope has substantiated that this phenomena occurs.

Because the outer shell freezes before the core, then the final frozen dropsize will be near that of the initial molten droplet. However, if it is desired to convert the measured data to the number of droplets, then it would be necessary to accurately determine the droplet density. The density will be different than that quoted for Shell 270 due to the hollow core.

To determine the limits of data reproducibility, two separate sets of experiments were conducted to measure dropsize over a range of injection velocity from about 70 to 150 ft/sec employing a like doublet injector. The results of these tests are presented in Table 3 and Fig. 13. The mass median dropsize was repeated to within ±3 percent as indicated by the dashed lines.

TABLE 3

FACILITY CHECKOUT AND DATA REPEATABILITY TESTS

Like Doublet Element
Orifice L/D = 10
Orifice Diameter = 0.063 Inch

Test No.	Wax Flowrate, lb/sec	Injection Velocity, ft/sec	Mass Median Dropsize, microns
1	0.150	72.5	413
2	0.162	78.1	415
3	0.207	100.1	337
4	0.227	110.0	303
5	0.268	129.9	256
6	0.309	149.7	223

TASK IA--PROPELLANT MISCIBILITY EFFECTS

The objective of this task was to determine the effect of miscibility on droplet size and dropsize distribution. The determination of the effect of miscibility on the atomization process is complicated by the large number of variables which could also affect these results. For instance, such parameters as the momentum level, orifice diameter ratio, and the dynamic pressure ratio can effect the atomization characteristics. It is important to select a liquid which is immiscible with wax but which has the proper physical properties. To separate these effects, where possible, the results for this task are discussed in three sections. In the first section, the rationale for the selection of a suitable immiscible liquid is presented. Then, the effects of miscibility on dropsize distribution for differing relative orifice diameters, momentum levels, and dynamic pressure ratios are presented. Finally, the effects of the same parameters on the mass median dropsize are discussed.

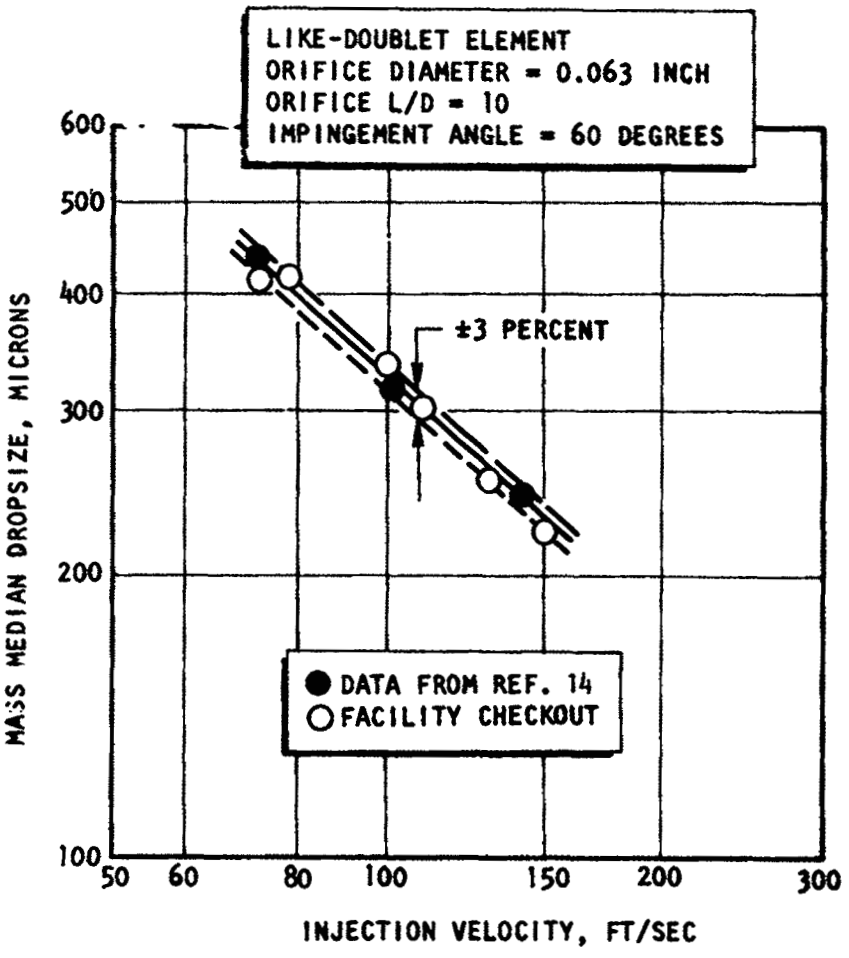

Figure 13. Results of Facility Checkout and Data Repeatability Tests

Selection of the Immiscible Liquid

At the outset of the program, a literature search was made to determine suitable liquids for use in the miscibility studies. It was considered desirable to use a wax immiscible liquid which possessed the same density, viscosity, and surface tension. This would allow a direct comparison of the effects of propellant miscibility on dropsize distribution. Several candidate liquids were evaluated, including water, glycols, ethanolamines, and various other amine compounds. However, no one compound or blend could meet all of the criteria. Assuming solubility and viscosity to be two of the more important factors, an aqueous solution containing approximately 75-percent diethanolamine appeared to be the best candidate. This mixture was found to be insoluble in the wax, has the same viscosity at 200 F, and has a density of about 1.0 gm/cc as compared to wax which is ~0.76 gm/cc. In addition, diethanolamine has the advantage of being nontoxic, compatible with aluminum and stainless steel, and is inexpensive. An alternate liquid that was considered was water thickened to increase the viscosity. For brevity, the diethanolamine-water mixture is henceforth referred to as DEW.

Dropsize Distribution

For these studies, three unlike-doublet injector elements having diameter ratios of 1.0, 1.36, and 2.03, and an impingement angle of 60 degrees were evaluated. To ensure that the free jet velocity profiles were symmetrical, long orifices (L/D = 50) with contoured entries were used. In all cases, the free jet length was maintained constant at 5 diameters.

A total of 29 experiments were conducted. The experiments were conducted such that the wax and the DEW were alternately used to simulate the fuel and the oxidizer. Therefore, when wax was used as the fuel simulant and DEW as the oxidizer simulant, the fuel-side droplet distribution was determined for the case of immiscible liquids. Combining the distributions obtained in individual tests for fuel and oxidizer gives the total, mass-weighted distribution and mass median dropsize ($\overline{D}$) under conditions of immiscibility.

It should be pointed out that, if the dynamic pressure ratio is such that the stream issuing from the larger orifices stagnates (i.e., has a smaller dynamic pressure than the other stream) against the other stream, then when the fluids are reversed the same larger orifice stream will still be the stagnating stream.

Because two separate tests are conducted, the proper ratio of masses must be used to obtain an overall distribution (corresponding to the input mixture ratio). The calculation procedure for obtaining the total dropsize and dropsize distribution is presented in Table 4.

TABLE 4

CALCULATION PROCEDURE FOR OBTAINING TOTAL DROPSIZE DISTRIBUTION FOR IMMISCIBLE IMPINGEMENT

Sieve Size, microns	Run No. 8		Run No. 11		Total Weighted Fraction	$\bar{D}$ = 348 microns	
	Mass Fraction	Weighted Fraction	Mass Fraction	Weighted Fraction		Cumulative Fraction	$D/\bar{D}$
Pan	0.0005	0.00026	0.0008	0.00038	0.00064	--	--
88	0.0020	0.00104	0.0017	0.00081	0.00185	0.00064	0.253
105	--	--	0.0048	0.00230	0.00230	0.00249	0.302
125	0.0035	0.00182	0.0074	0.00354	0.00536	0.00479	0.359
149	0.0180	0.00938	0.0369	0.01768	0.02706	0.01015	0.428
177	0.0414	0.02157	0.0434	0.02079	0.04236	0.03721	0.509
210	0.1045	0.05444	0.1054	0.05049	0.10493	0.07957	0.604
250	0.1472	0.07669	0.1412	0.06763	0.14432	0.18450	0.719
297	0.2014	0.10493	0.1764	0.08450	0.18943	0.32882	0.854
354	0.2560	0.13338	0.1876	0.08986	0.22324	0.51825	1.017
420	0.1503	0.07830	0.1375	0.06586	0.14416	0.74149	1.207
500	0.0628	0.03272	0.1176	0.05633	0.08905	0.88565	1.437
590	0.0082	0.00427	0.0392	0.01878	0.02305	0.97470	1.696
710	0.0042	0.00219	--	--	0.00219	0.99775	2.040

For the case of miscible impingement, a third experiment was conducted utilizing molten wax as the simulant for both fuel and oxidizer. This experiment, which was conducted at approximately the same total jet momentum level, as in the preceding immiscible tests, gives directly the overall distribution for miscible impingement.

The results for each experiment conducted are presented in Table 5. All pertinent geometric, hydraulic, and dynamic parameters are included. The last column in the table is the mixing uniformity (ϕ) defined by Rupe (Ref. 16) as:

$$\phi = \frac{1}{1 + \frac{\rho_1 V_1^2 d_1}{\rho_2 V_2^2 d_2}}$$

where

ρ = propellant density

V = injection velocity

d = orifice diameter

Note that the subscripts 1 and 2 refer to the respective propellant systems as labeled in the table. This could be somewhat confusing in that the momentum ratio (M_1/M_2) or dynamic pressure ratio (P_{T_1}/P_{T_2}) is not always the wax/DEW ratio. For each test, the mass median dropsize of the orifice or orifices flowing are presented in the last column. The three unlike doublet injector elements were each flowed at three momentum levels ($\dot{w}_{ox}V_{ox} + \dot{w}_f V_f$) of 7, 20, and 40 ft-lb/sec^2. Insufficient freezing of the wax drops using the 2.03 diameter ratio element invalidated the data obtained at the low momentum level of 7 ft-lb/sec^2; hence; this data point was not included in Table 5.

TABLE 5

TASK IA MISCIBILITY RESULTS

Run No.	Diameter Ratio	System No. 1 (Wax) Orifice Diameter, inch	System No. 1 (Wax) Flowrate, lb/sec	System No. 1 (Wax) Velocity, ft/sec	System No. 2 (Wax or Dew) Simulant	System No. 2 (Wax or Dew) Orifice Diameter, inch	System No. 2 (Wax or Dew) Flowrate, lb/sec	System No. 2 (Wax or Dew) Velocity, ft/sec	Momentum Ratio, M_1/M_2*	Total Momentum, ft-lb/sec^2	Dynamic Pressure Ratio,* P_{T1}/P_{T2}	Measured $\bar{D}$, microns	Mixing Uniformity Parameter (ϕ)
1	1.0	0.063	0.0582	56.3	Dew	0.063	0.0723	52.2	0.87	7.05	0.87	339	0.536
2		0.063	0.0906	87.7	Dew	0.063	0.1210	87.4	0.75	18.52	0.75	290	0.570
3		0.063	0.1440	139.3	Dew	0.063	0.1728	124.8	0.93	41.62	0.93	257	0.518
4		0.063	0.0555	53.7	Wax	0.063	0.555	53.7	1.0	5.96	1.0	369	0.500
5		0.063	0.1017	98.4	Wax	0.063	0.1017	98.4	1.0	20.01	1.0	276	0.500
6		0.063	0.1475	142.7	Wax	0.063	0.1475	142.7	1.0	42.10	1.0	238	0.500
7	1.36	0.063	0.0614	59.4	Dew	0.086	0.0883	34.3	1.20	6.68	2.24	443	0.378
8		0.063	0.1175	113.7	Dew	0.086	0.1473	57.1	1.59	21.77	2.96	349	0.316
9		0.063	0.1545	149.5	Dew	0.086	0.2097	81.3	1.35	40.15	2.52	274	0.350
10		0.086	0.0840	43.6	Dew	0.063	0 0854	61.7	0.70	8.93	0.37	434	0.659
11		0.086	0.1080	56.1	Dew	0.063	0.1279	92.4	0.51	17.88	0.28	346	0.727
12		0.086	0.1782	92.6	Dew	0.063	0.1663	120.1	0.83	36.47	0.44	294	0.624
13		0.086	0.0761	39.5	Wax	0.063	0.0637	61.6	0.77	6.93	0.41	453	0.641
14		0.086	0.1241	64.5	Wax	0.063	0.1066	103.1	0.73	18.99	0.39	384	0.653
15		0.086	0.1807	93.9	Wax	0.063	0.1519	147.0	0.76	39.30	0.41	302	0.643
16		0.063	0.0457	44.2	Dew	0.086	0.0861	33.4	0.70	4.90	1.31	384	0.510
17		0.063	0.0894	86.5	Dew	0.086	0.1741	67.5	0.66	19.59	1.23	321	0.526
18		0.063	0.1277	123.6	Dew	0.086	0.2465	95.6	0.67	39.35	1.25	291	0.521
19		0.063	0.0465	45.0	Dew	0.086	0.1159	45.0	0.40	7.31	0.75	421	0.646
20		0.063	0.0826	79.9	Dew	0.086	0.2105	81.7	0.38	23.80	0.71	352	0.656
21		0.063	0.1126	109.0	Dew	0.086	0.2545	98.7	0.49	37.39	0.91	292	0.600
22	2.03	0.063	0.0805	77.9	Wax	0.128	0.2293	53.8	0.51	18.61	2.10	499	0.493
23		0.063	0.1203	116.3	Wax	0.128	0.3430	80.5	0.51	41.62	2.09	457	0.492
24		0.063	0.0467	45.2	Dew	0.128	0.1583	29.5	0.43	7.08	1.75	558	0.536
25		0.063	0.0856	82.9	Dew	0.128	0.2865	53.4	0.44	23.39	1.80	375	0.530
26		0.063	0.1162	112.5	Dew	0.128	0.3740	69.7	0.47	40.83	1.95	272	0.512
27		0.128	0.1455	34.1	Dew	0.063	0.0559	43.0	0.51	7.53	0.48	591	0.511
28		0.128	0.2445	57.4	Dew	0.063	0.0924	71.1	0.50	21.02	0.48	538	0.504
29		0.128	0.3620	84.9	Dew	0.063	0.1330	102.4	0.47	45.24	0.51	448	0.490

Unlike-Doublet Elements; Free Jet Length = 5 Diameters; Impingement Angle = 60 Degrees; Orifice L/D = 50

*Subscripts 1 and 2 refer to the respective propellant systems

$$\phi = \frac{1}{1 + \frac{\rho_1 V_1^2 d_1}{\rho_2 V_2^2 d_2}}$$

It was initially intended to conduct all of the tests at the uniformity mixing conditions defined by Rupe (Ref. 16). Because of an error in the flow calculations, a number of tests were made at non-optimum flow conditions. Examination of Table 5 shows this to be true for the 1.36 diameter ratio element (with the exception of tests 16 through 18). However, the experiments conducted with the 1.0 and 2.03 diameter ratio elements (tests 1 through 6, and 22 through 29, respectively) were made at or near the optimum mixing value.

Diameter Ratio and Momentum Level Effects. The basic data obtained to determine the influence of diameter ratio and momentum level are presented in Fig. 14, 15, and 16. In Fig. 14 the cummulative mass fraction as a function of the droplet size normalized by dividing by the mass median dropsize for several momentum levels are presented for the case of immiscible (wax/DEW) and miscible (wax/wax) flow. These data were obtained utilizing an equal diameter unlike-doublet. Consequently, for these experiments the dynamic pressure ratio is nearly one. In addition, because the dynamic pressure ratio is almost unity and the orifice sizes are equal, then the dropsize distribution determined for the orifice flowing wax is representative of the overall spray dropsize distribution. It is obvious from inspection of Fig. 14 that momentum level had no discernible affect on dropsize distribution.

The data presented for the 1.0 and 2.03 diameter ratio elements (Fig. 14 and 16, respectively) can be used directly to determine if miscibility has an effect on the dropsize distribution. The data obtained for the 1.36 diameter ratio element (Fig. 15) cannot be utilized because test conditions did not correspond to the uniform mixing conditions. For the equal diameter results shown in Fig. 14 it is only necessary to compare the distribution curves shown in the upper plot obtained with wax flowing in one orifice and the immiscible fluid DEW in the other with the lower curve obtained with wax flowing in both orifices (miscible). For the unequal diameter orifices, it is first necessary to combine the distributions obtained from both the large and the small orifice to obtain the overall

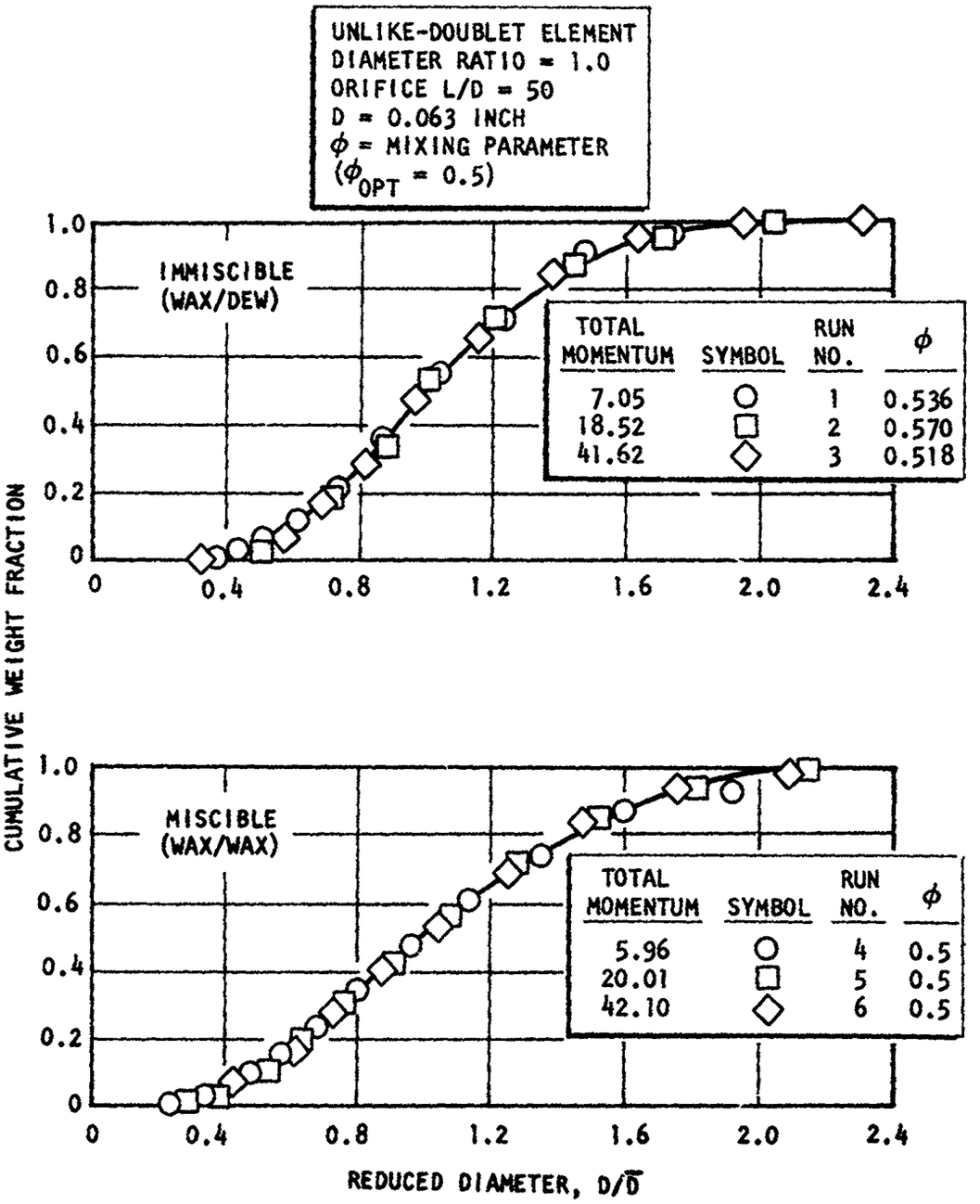

Figure 14. Normalized Distribution Curves for an Unlike-Doublet Element Having a Diameter Ratio of 1.0

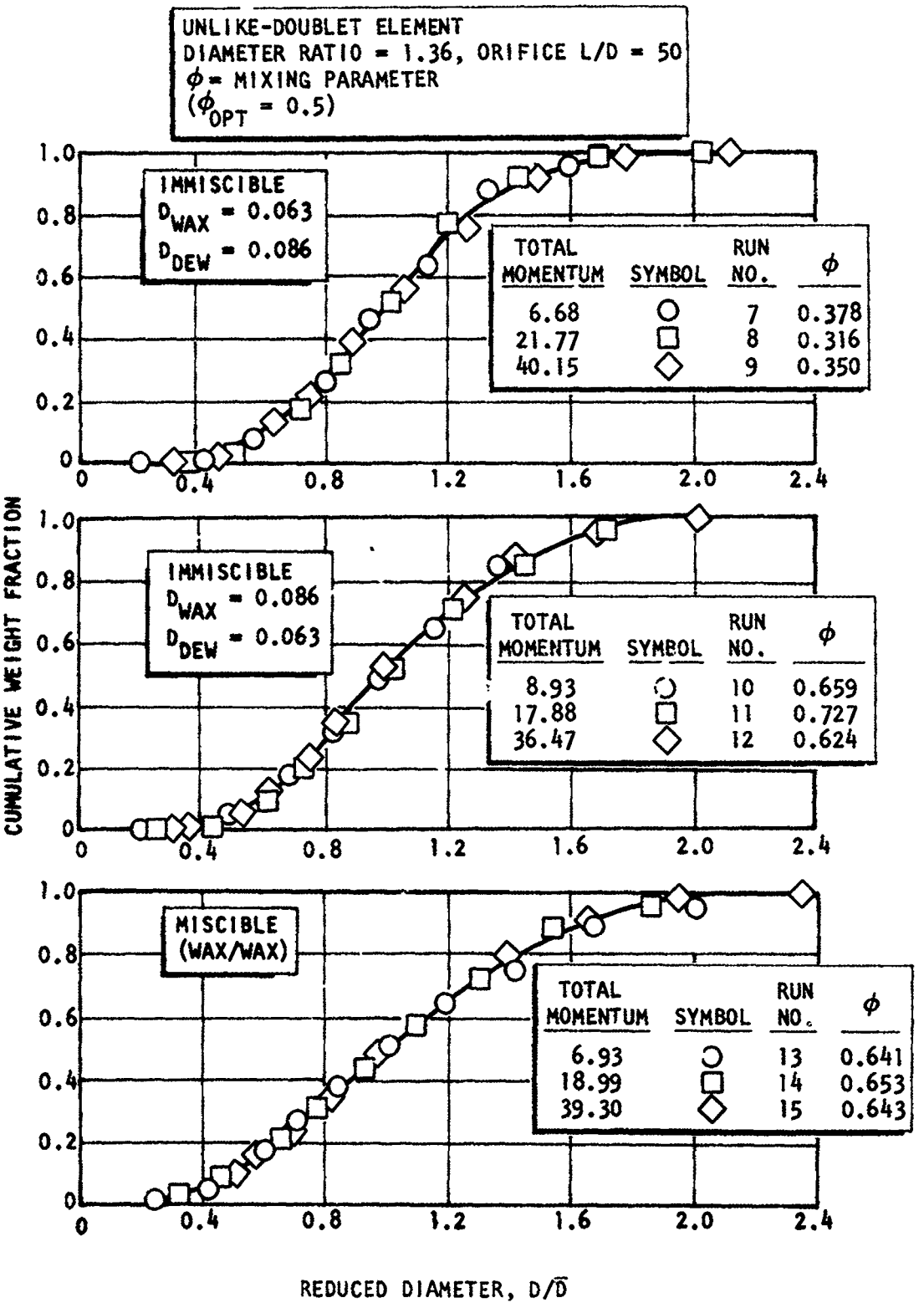

Figure 15. Normalized Distribution Curves for an Unlike-Doublet Element Having a Diameter Ratio of 1.36

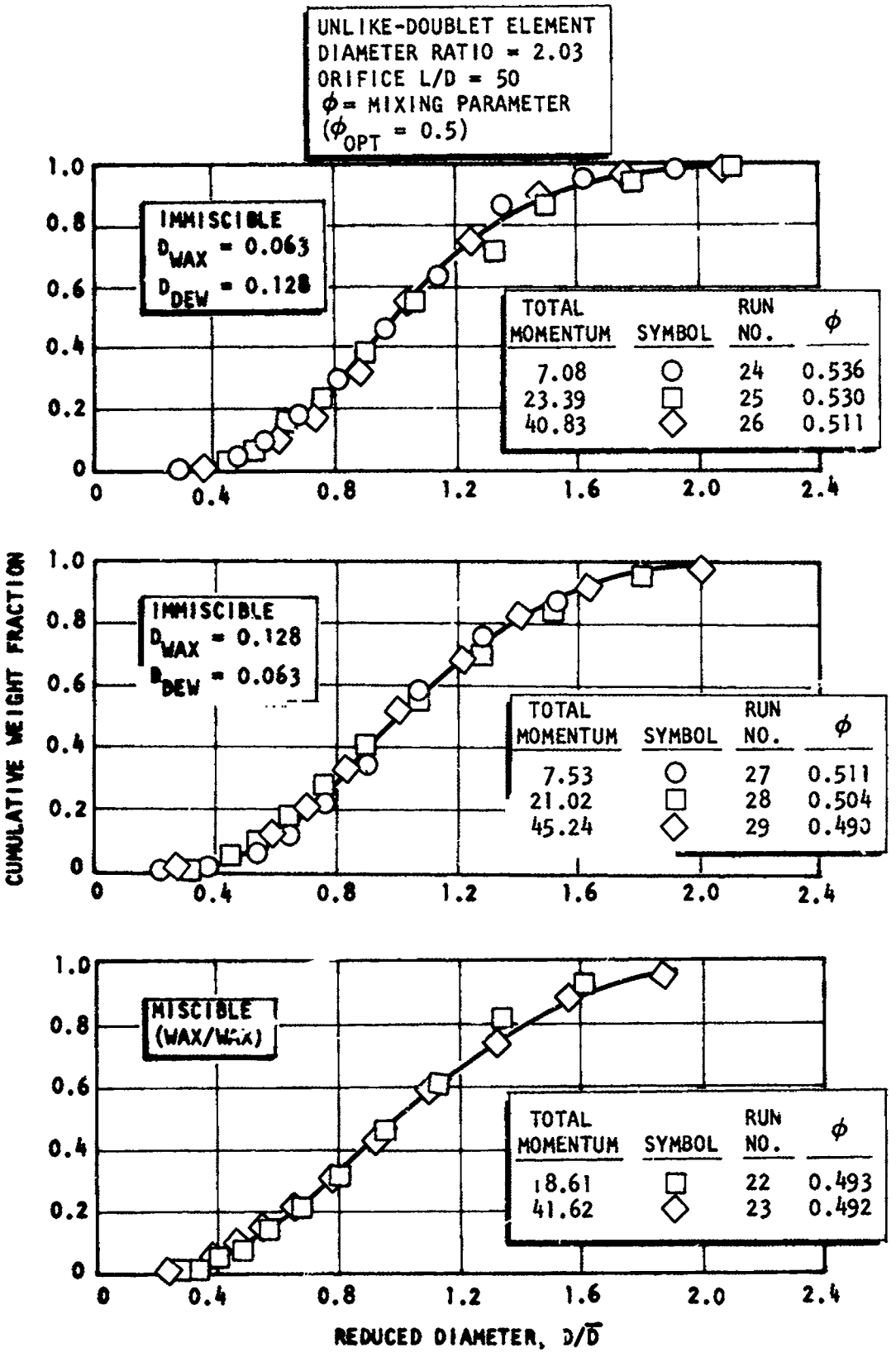

Figure 16. Normalized Distribution Curves for an Unlike-Doublet Element Having a Diameter Ratio of 2.03

distribution. This result can then be directly compared to the overall distribution shown in the lower curve obtained at near identical flow conditions and consequently nearly identical dynamic pressure ratio with wax flowing in both orifices. This was done for the 1.0 and 2.03 diameter ratio elements and the results are presented in Fig. 17. These results show that miscibility has an effect on the dropsize distribution. In addition, the condition of immiscibility results in a distribution closer to the monodisperse case (all droplets at one diameter) than does miscible impingement.

A comparison of the miscible curves for the 1.0 and 2.03 diameter ratio unlike-doublet elements is shown in Fig. 18; the immiscible results are shown in Fig. 19. Examination of these two figures shows that the effects of diameter ratio were small and approximately the same for both miscible and immiscible impingement.

Examination of the dropsize distribution obtained with the unequal diameter ratio elements, Fig. 15 and 16, shows that the distributions obtained for the large and the small diameter orifice were different. This is illustrated in Fig. 20. (It should be noted that the magnitude of the differences in the distributions are in agreement with those found in the Ref. 14 study.) This difference in the distribution characteristics between the larger and smaller diameter orifices can be attributed to either diameter ratio effects or the fact that, in all of the unequal diameter experiments, the larger of the two streams was stagnated (i.e., the larger stream had a lower stagnation pressure) and should therefore produce differing characteristics. Based upon physical arguments, it would be expected that the larger diameter orifice would produce a greater number of droplets of large diameter than the smaller orifice because part of the larger jet does not come into direct contact with the smaller jet at initial impingement. Examination of the results shown in Fig. 20 shows that for both the 1.36 and 2.03 diameter ratio elements, the larger stream produces a greater number of larger droplets even though the mixing quality was significantly

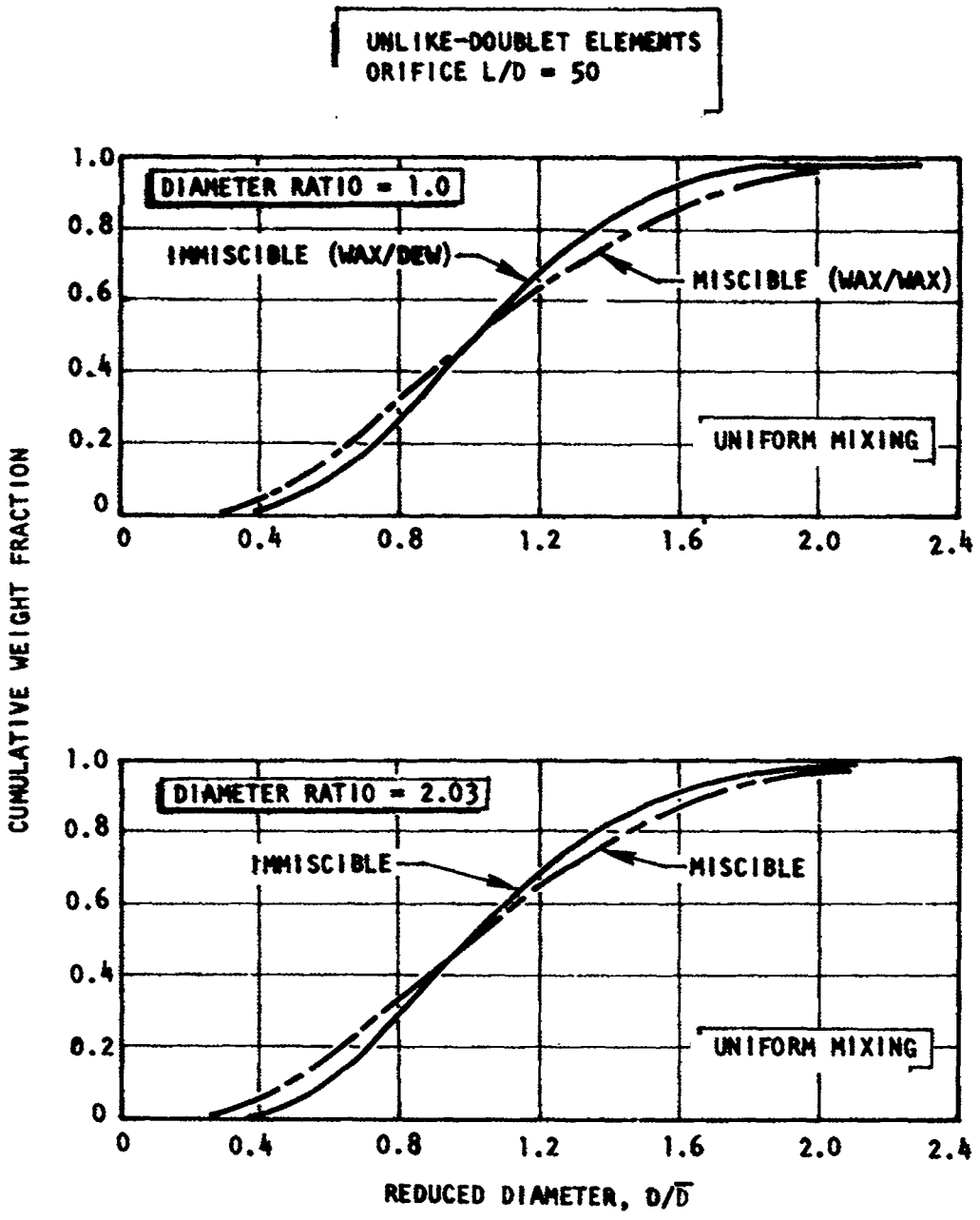

Figure 17. Normalized Distribution Curves for Miscible and Immiscible Impingement Using Unlike-Doublet Injection Elements

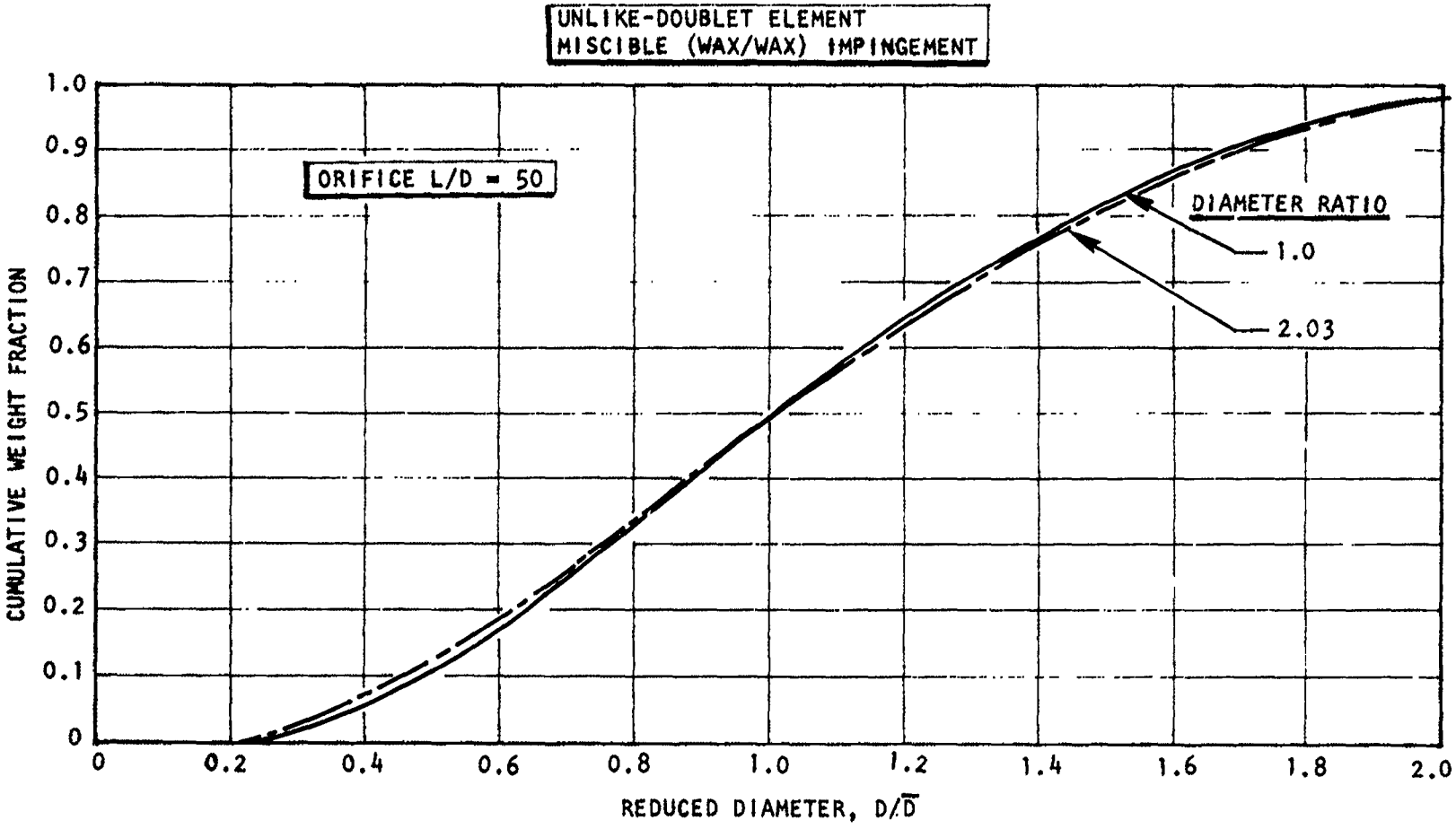

Figure 18. Normalized Distribution Curves Obtained for the Case of Miscible (Wax/Wax) Impingment

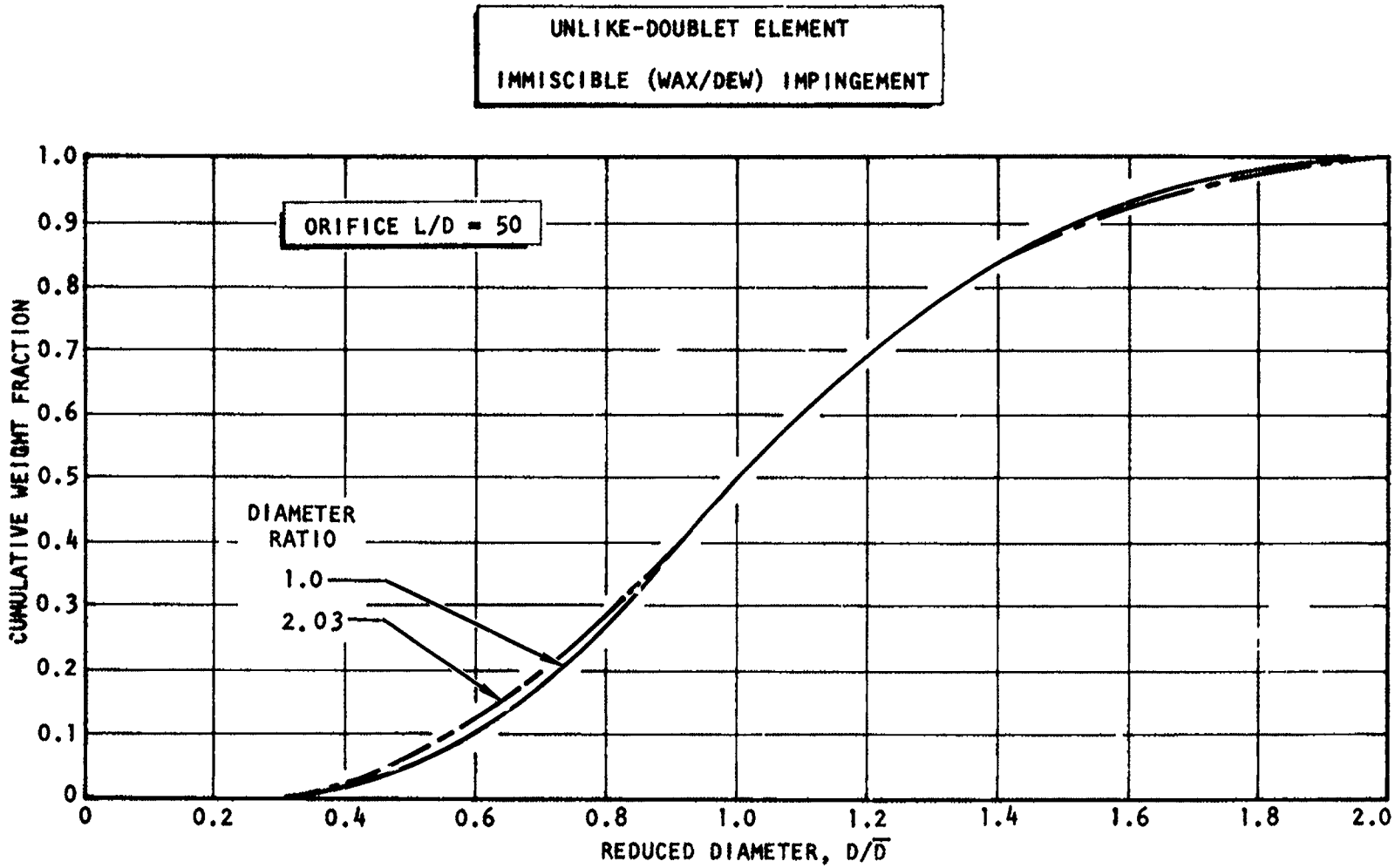

Figure 19. Normalized Distribution Curves Obtained for the Case of Immiscible (Wax/Dew) Impingement

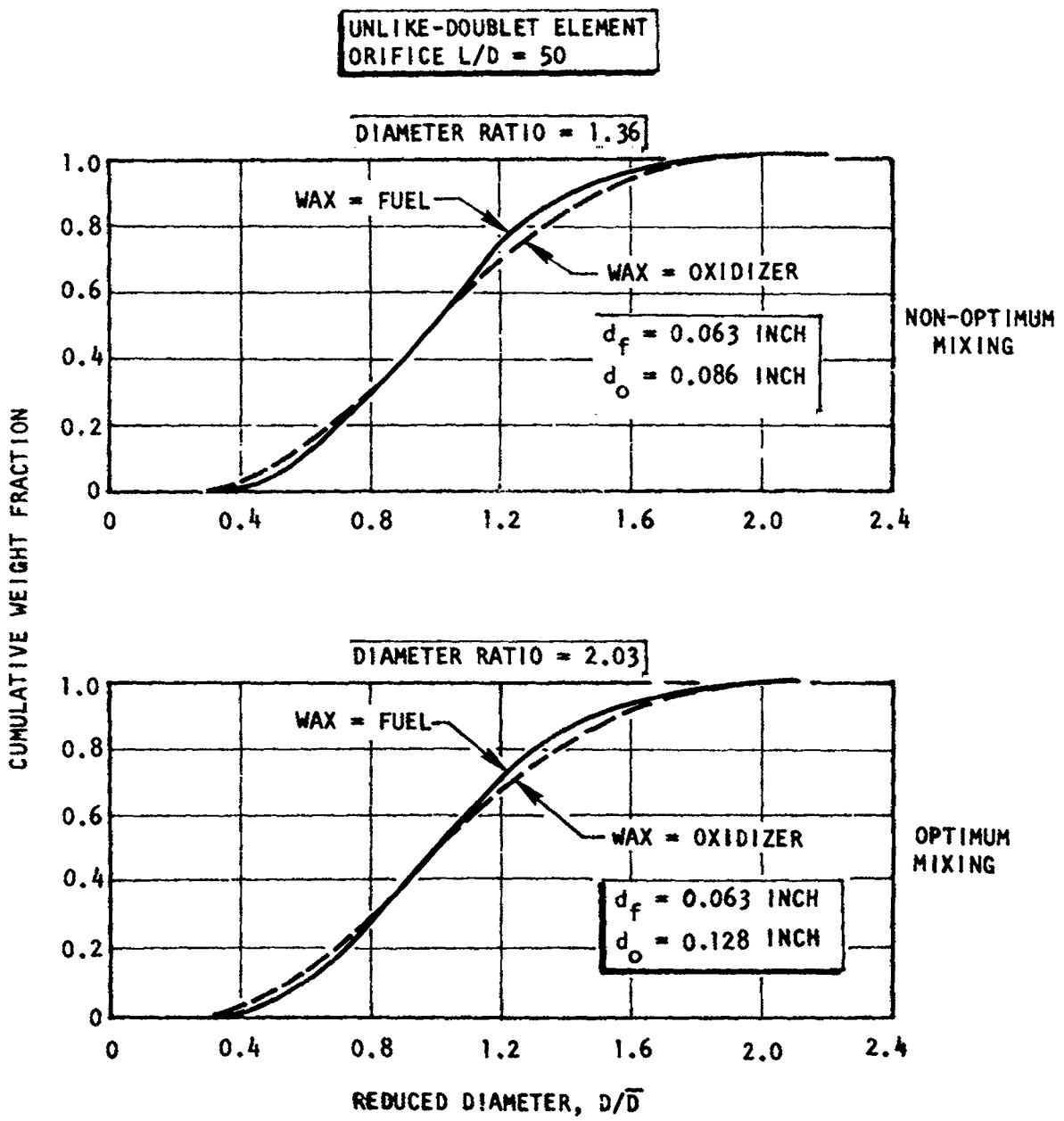

Figure 20. Fuel and Oxidizer Distribution Curves for Unlike-Doublet Elements Having Unequal Orifice Diameters

different for the two cases. This suggests that the difference in distributions is caused by diameter ratio. However, the data are not sufficient to verify whether diameter ratio or the stagnation of one stream produced the differences in the distribution.

Dynamic Pressure Ratio Effects. Six wax experiments were conducted utilizing the 1.36-diameter ratio element with the wax simulating the fuel ($d_f < d_o$), tests No. 16 through 21, Table 4. The addition of these data with the previous immiscible, fuel-side experiments (runs 7 through 9) provided a comparison of the effect of dynamic pressures on the fuel dropsize. The experimental distribution data are plotted in Fig. 21. For each dynamic pressure ratio the total momentum of the streams was varied. It should be noted, however, that in varying the dynamic pressure ratio, the mixing parameter is also changed. (As discussed earlier, it was found that momentum level has no effect on the dropsize distributions.) A comparison of the average distribution curves for these three cases is shown in Fig. 22. These results show that the dynamic pressure ratio has a small effect on dropsize distribution. It should be noted that, for the nominal dynamic pressure ratios of 1.26 and 2.57, the oxidizer (large) stream is stagnated, whereas, at 0.79, the fuel (smaller) stream is stagnated. These results show that the distributions are different for each dynamic pressure ratio evaluated. This suggests that for each flow condition with unequal dynamic pressure ratios no universal distribution curve exists. Therefore, each flow condition will have a unique dropsize distribution.

Mass Median Dropsize

To more fully describe the miscible and immiscible spray characteristics, a statistical mean or median dropsize is required in addition to the distribution curve. The two most commonly used dropsizes are the mass median ($\bar{D}$) and the volume mean (D_{30}). For this program the mass median dropsize was selected for the following reasons. First, the sieve analysis of the frozen wax droplets yields the overall size distribution from which the mass median is easily calculated. Second, the volume mean dropsize is

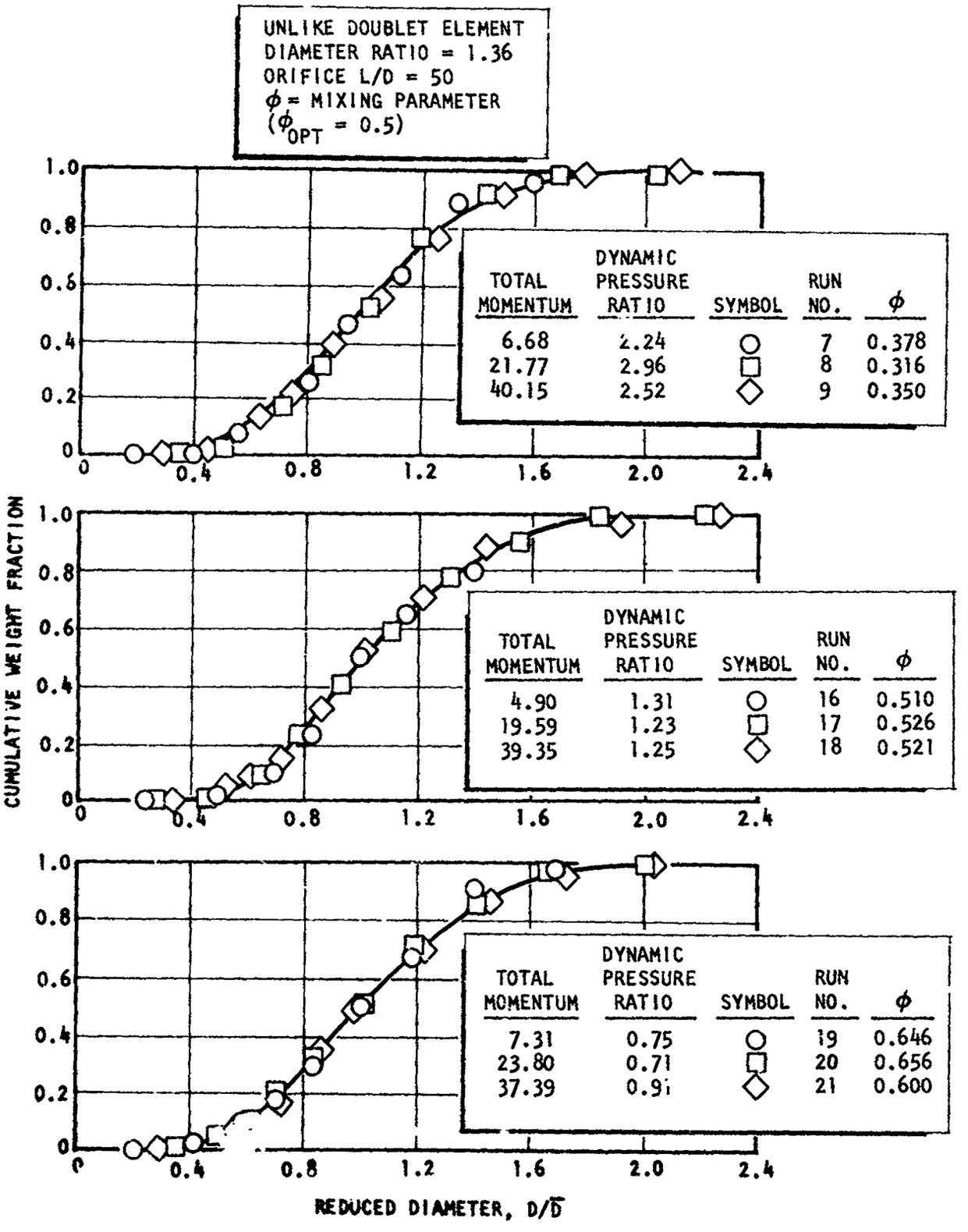

Figure 21. Normalized Distribution Curves for Unlike-Doublet Element at Various Momentum Levels and Dynamic Pressure Ratios

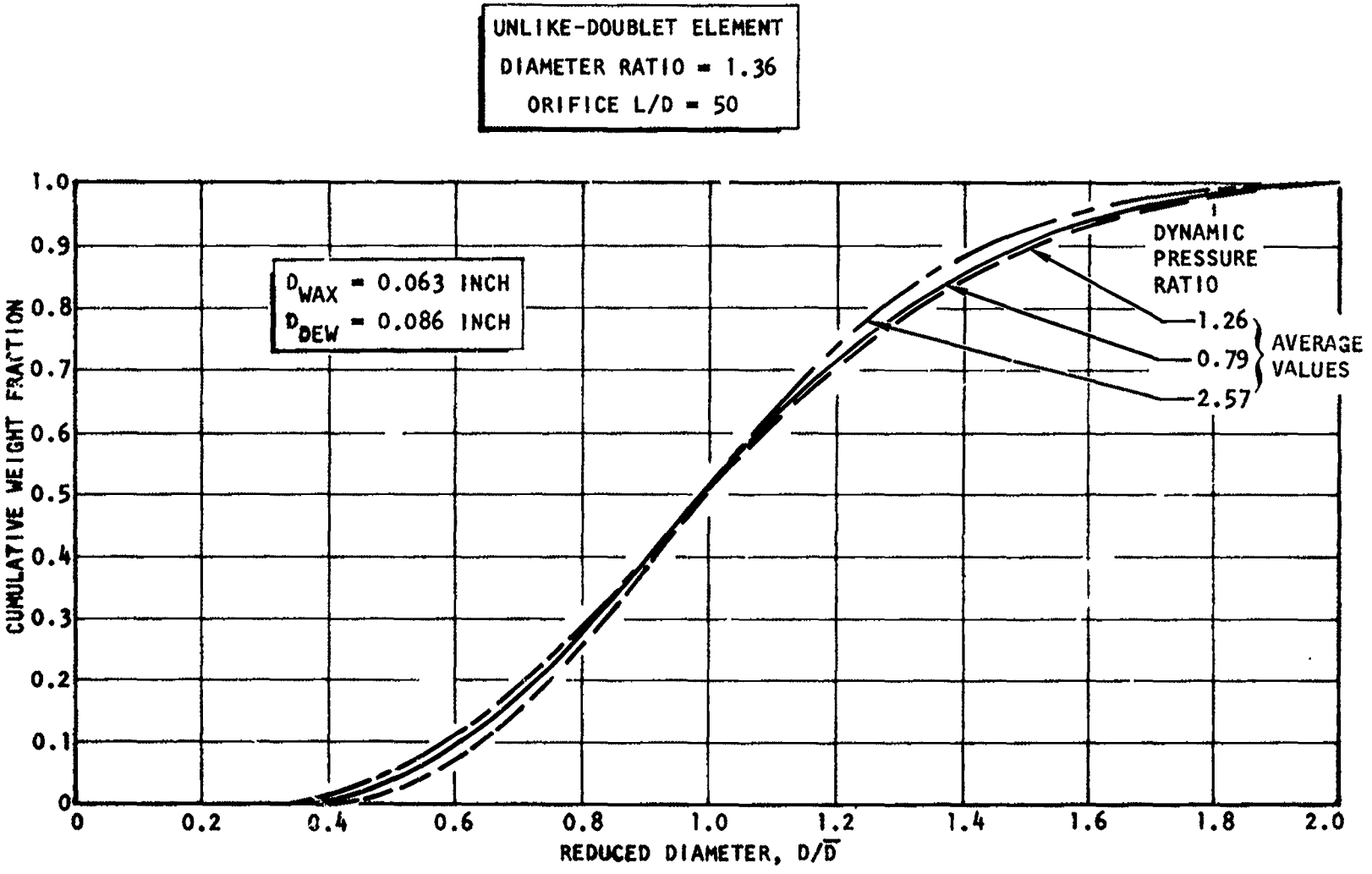

Figure 22. Normalized Distribution Curves for an Unlike-Doublet Element at Three Dynamic Pressure Ratios

dependent upon the shape of the distribution curve, particularly at the lower end of the distribution curve. The mass median size, however, is basically independent of the shape of the distribution curve, a condition which allows for an independent comparison of the spray size and distribution characteristics.

Miscibility Effects on Dropsize. The influence of miscibility on dropsize is most easily shown by comparison of the mass median dropsizes obtained for equal diameter jets, wherein wax was flowed through both orifices and then when wax and DEW were flowed through the orifices. For this case both the orifice diameter, velocity, and dynamic pressure ratios are equal to 1.0. These results are compared in Fig. 23. It is evident that under conditions of equal injection velocity the same size drops are produced for miscible and the immiscible impingement.

The correlating equations presented in Ref. 14 for like doublets and unlike doublets are as follows:

$$\text{Like Doublet:} \qquad \overline{D} = 7.8 \times 10^{4} \left[\frac{D^{0.57}}{V^{0.85}}\right]$$

$$\text{Unlike Doublet:} \qquad \overline{D}_f = 1.0 \times 10^{5} \left[\frac{D_f^{0.27}\, D_o^{0.023}}{V_f^{0.74}\, V_o^{0.33}}\right]$$

where

D = orifice diameter, inch

V = injection velocity, ft/sec

and the subscripts f and o refer to fuel and oxidizer, respectively.

Substitution into these equations shows that in the range of injection velocity from 100 to 150 ft/sec, and for an orifice diameter of 0.063

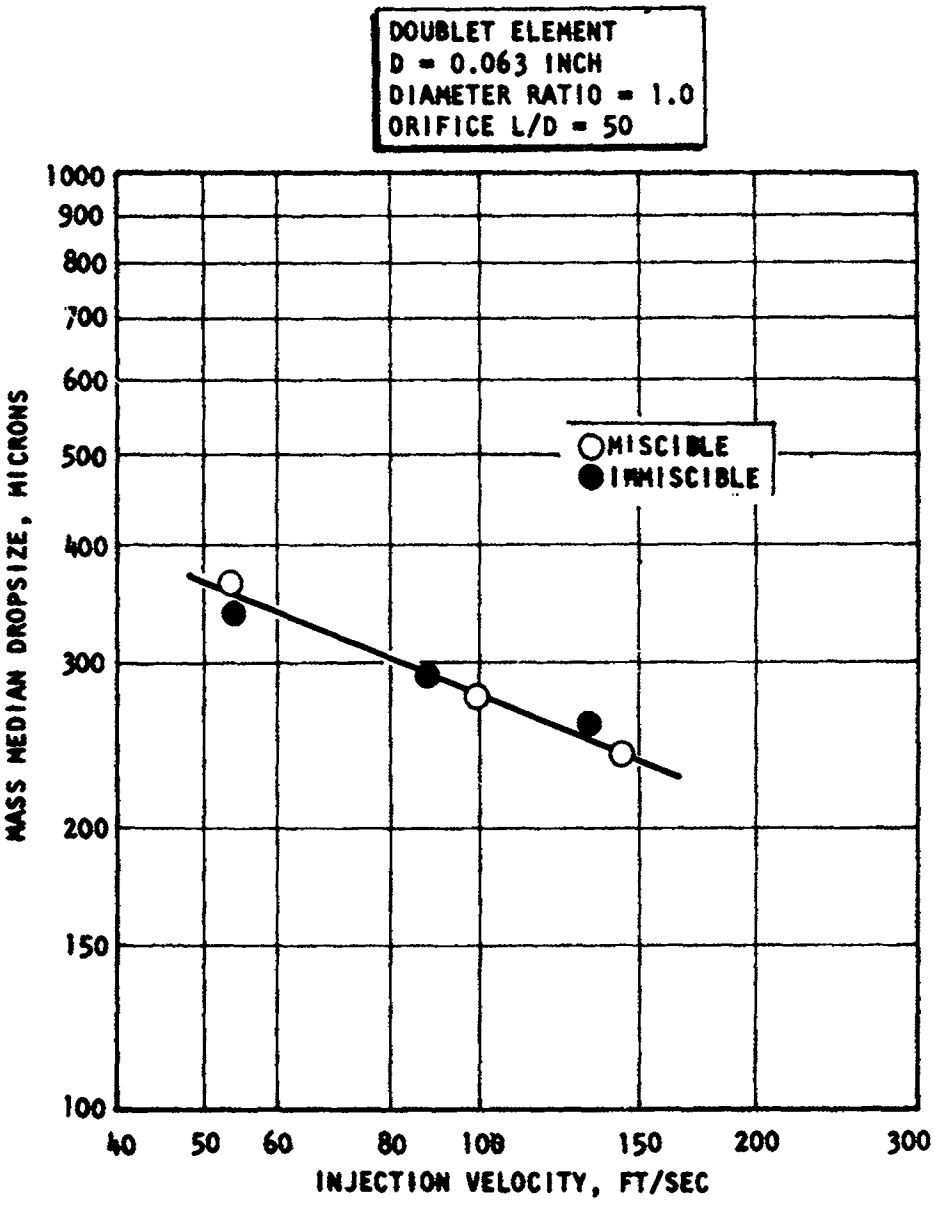

Figure 23. Comparison of Mass Median Dropsizes for Miscible and Immiscible Impingement

inch, the two equations agree within ~10 percent. Examination of the two equations reveals that, because of the differing exponents of orifice diameter and injection velocity, unequal dropsizes will be predicted at other values of orifice diameter and velocity. It should be noted, however, that these dropsize correlations were obtained near the rather narrow range of only about 100 to 150 ft/sec.

Diameter Ratio Effects

The mass median dropsizes obtained for the unequal diameter ratio unlike-doublet elements are shown in Table 6. The results are shown in tabular form because the miscible and immiscible injection velocities were not identical. The velocities in the table thus represent the average of the miscible and immiscible velocities. As shown in Table 6, the mass median dropsize $\bar{D}_1$ and $\bar{D}_2$ are different for each jet as was the dropsize distribution. It is interesting to note that the magnitude of the difference between the individual dropsizes is much greater for the larger diameter ratio element. However, the data were not obtained at flow conditions such that a direct comparison of the influence of diameter ratio or velocity can be made. Also included in the table for each test are the overall mass weighted average dropsizes for the entire spray. This average dropsize obtained for the immiscible case is compared with the average spray dropsize obtained for the miscible experiments. Note that small differences do occur but this variation is within the accuracy of the data.

Dynamic Pressure Ratio Effects. The fuel-side dropsize data obtained in the 1.36 diameter ratio tests are presented in Fig. 24. The upper plot shows the fuel dropsize as a function of the uniformity mixing parameter defined by Rupe (Ref. 16). The data are also presented as a function of the dynamic pressure ratio in the lower plot.

The data show a definite trend toward minimum dropsize at the low momentum levels. This trend was not observed at the highest momentum investigated (40 ft-lb/sec^2).

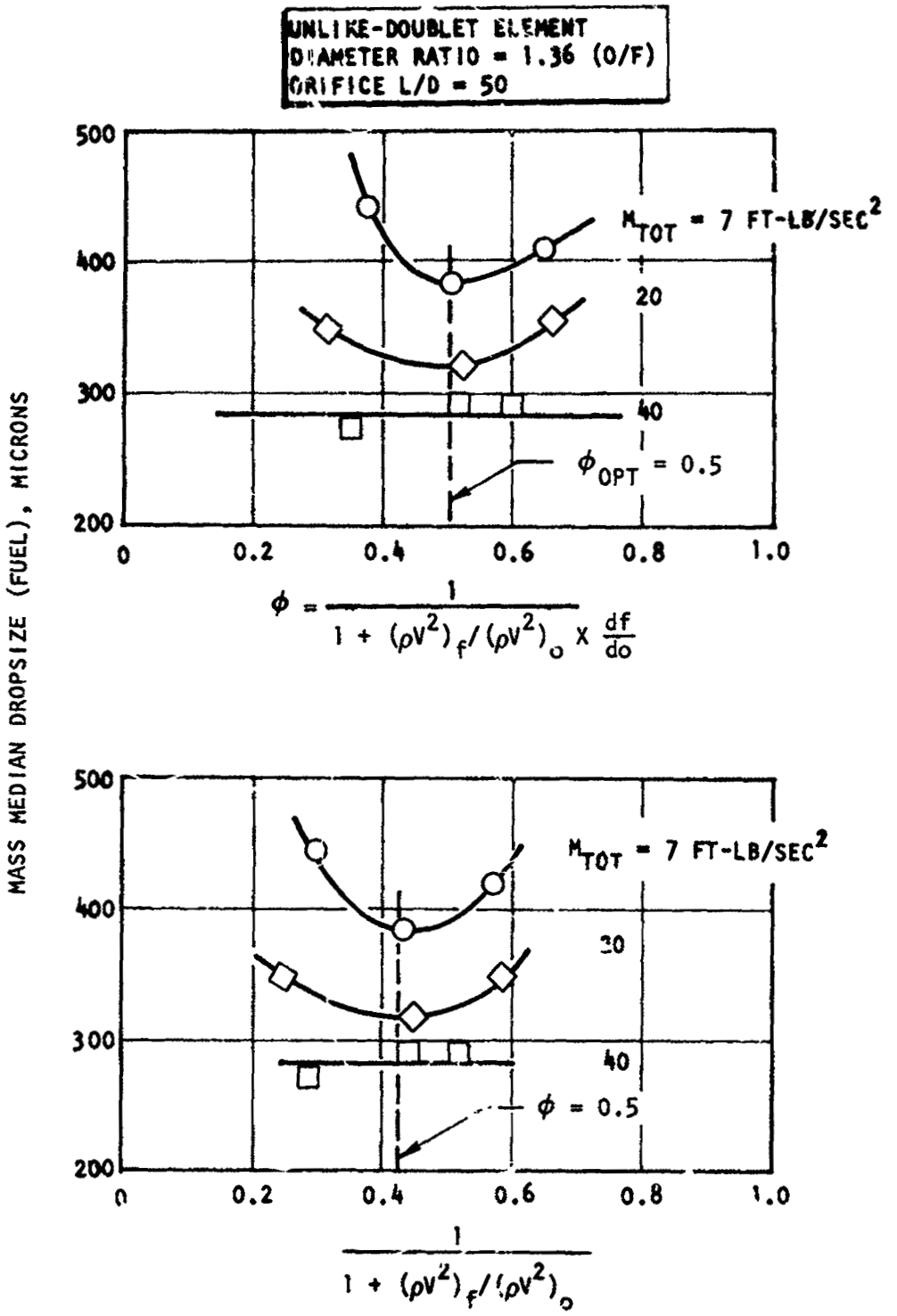

Figure 24. Fuel Dropsize vs Unif .mity Mixing Parameter and Dynamic Pressure Ratio for an Unlike Doublet Element

TABLE 6

COMPARISON OF MISCIBLE AND IMMISCIBLE DROPSIZES FOR UNEQUAL DIAMETER ELEMENTS*

D_1, inch	D_2, inch	Average** V_1, ft/sec	Average** V_2, ft/sec	$\bar{D}_1$, microns	$\bar{D}_2$, microns	Mass Weighted $\bar{D}$, microns	Miscible $\bar{D}$, microns	Mixing
0.063	0.086	60	41	443	434	438	453	Nonuniform
↓	↓	108	60	349	346	348	384	↓
↓	↓	148	93	274	294	285	302	↓
↓	0.128	45	34	558	591	583	--	Uniform
↓	↓	80	55	375	538	496	499	↓
↓	↓	115	83	272	448	405	457	↓

*Immiscible and miscible experiments conducted at same operating conditions of velocity and mixture ratio.

**Average $V = (V_{miscible} + V_{immiscible})/2$

Although only a limited amount of data was obtained, it would appear that the minimum dropsize occurs at the point of uniform mixing ($\phi = 0.5$ in the upper plot of Fig. 24). It should be noted that, for an unlike doublet element having unequal diameter orifices, the conditions of equal dynamic pressure and uniform mixing do not occur simultaneously because

$$\text{Mixing Parameter} = \text{Dynamic Pressure Ratio} \times \text{Diameter Ratio}$$

$$= (\rho V^2)_f/(\rho V^2)_o \times \frac{d_f}{d_o}$$

In order to determine which of the two parameters is the more significant in producing the minimum dropsize, it would be necessary to utilize a larger diameter ratio. For example, at a diameter ratio of 2.0 (o/f), the level of $\phi = 0.5$ corresponds to a value of the parameter $1/(1+\rho_f V_f^2/\rho_o V_o^2)$ of 0.33.

TASK IB--OCCURRENCE OF EMULSIFICATION

The objective of this task is to determine if an emulsion is formed at the interface of two jets flowing immissible fluids. Because unlike impinging elements are designed such that the liquid fuel and oxidizer impinge with considerable dynamic force, it is conceivable that an emulsion may be formed. The occurrence of an emulsion at the interface would be extremely important to any model describing mixing, atomization, or reactive stream blowapart. A detailed description of the experimental method for the quantitative determination of the extent of emulsification was given in the Experimental Procedure Section. Described below are (1) experiments conducted to verify that the quantitative measurements of emulsification were indeed the result of the amount of one propellant entrapped within a droplet of the other, and (2) the results of the emulsification experiments.

Verification Tests

Molten wax and the diethanolamine-water (DEW) mixture were used as propellant simulants in this study. The frozen wax particles resulting from unlike element tests were collected and thoroughly washed in water to e-move any traces of diethanolamine (DEA) which might have adhered to the outside of the spherical particles. The quantity of remaining DEA contained in the wax was determined by mixing the wax with an equal amount of water, heating the mixture to the melting point of the wax, and allowing the mixture to separate. The amount of DEA originally included in the wax was then determined by a chromatographic analysis of the DEA-water mixture. A question was raised as to the effectiveness of the removal of DEA from the surface of the droplets. As discussed below, the amounts of DEA measured were small and consequently small amounts of DEA left on the surface of the droplet would have a large affect on the interpretation of the results. A controlled test was therefore conducted wherein wax droplets uncontaminated with DEA (formed from wax on wax impingement) were subjected to a DEA-H_2O solution for a period of 12 days. The droplets were then given the identical washing procedure as that for the emulsification

tests. The wax was then subjected to chromatographic analysis to determine the amount of DEA in the droplets. The results of this analysis showed that no detectable amount of DEA was present in the washed sample. This result verifies that the experimental procedure for washing of the wax droplets is sufficient to remove the DEA from the surface. Therefore, any DEA that is measured in subsequent experiments was indeed entrapped within the wax droplet and not on the surface.

Quantitative Measurement of Emulsification

It was postulated that the amount of emulsification occurring would be different for each injector element type and momentum level. Therefore, experiments were conducted to determine the emulsification characteristics over a range of momenta level employing both an unlike doublet and unlike pentad element injector. The unlike-doublet element incorporated a 1.36 diameter ratio, and the 4-on-1 pentad element had a D_f/D_{ox} of 2.03 (four outer streams impinging on a central stream).

A total of six tests were conducted; three each for the two injector types. The experiments were conducted over a total injected momentum level of from about 7 to 50 ft-lb_m/sec^2.

The tests were conducted at nominal fuel/oxidizer momentum ratios of 0.42 and 0.98 for the unlike-doublet and pentad elements, respectively. The latter value corresponds closely to the condition of optimum mixing for the pentad (optimum value = 0.82) whereas for the unlike doublet, due to a calculational error, the flow conditions were significantly off the optimum value of 0.73.

The data are summarized in Table 7.

The results presented in Fig. 25 show a nominal level of 1-percent DEW imbedded in the wax droplets for both the unlike doublet and pentad elements. A repeat chromatographic analysis of the unlike-doublet droplets

TABLE 7

TASK IB EMULSIFICATION RESULTS

Task I Run No.	Element Type	Wax System			Dew System			Total Momentum, ft-lb/sec^2	$\frac{M_{wax}}{M_{Dew}}$	Percent Dew in Wax
		Orifice Diameter, inch	Flowrate, lb/sec	Injection Velocity, ft/sec	Orifice Diameter, inch	Flowrate, lb/sec	Injection Velocity, ft/sec			
19	Unlike-Doublet	0.063	0.0465	45.0	0.086	0.1159	45.0	7.31	0.40	0.67
20	↓	0.063	0.0826	79.9	0.086	0.2105	81.7	23.80	0.38	1.20
21	↓	0.063	0.1126	109.0	0.086	0.2545	98.7	37.39	0.49	0.84
30	Pentad	0.128	0.0856	20.1	0.063	0.1839	44.5	9.91	0.84	0.93
31	↓	0.128	0.1482	34.8	0.063	0.2988	72.3	26.76	0.95	0.67
32	↓	0.128	0.2189	51.4	0.063	0.4030	97.5	50.54	1.15	1.00

NOTE: Orifice L/D = 50
Free Jet Length = 5 diameters
Impingement Angle = 60 degrees

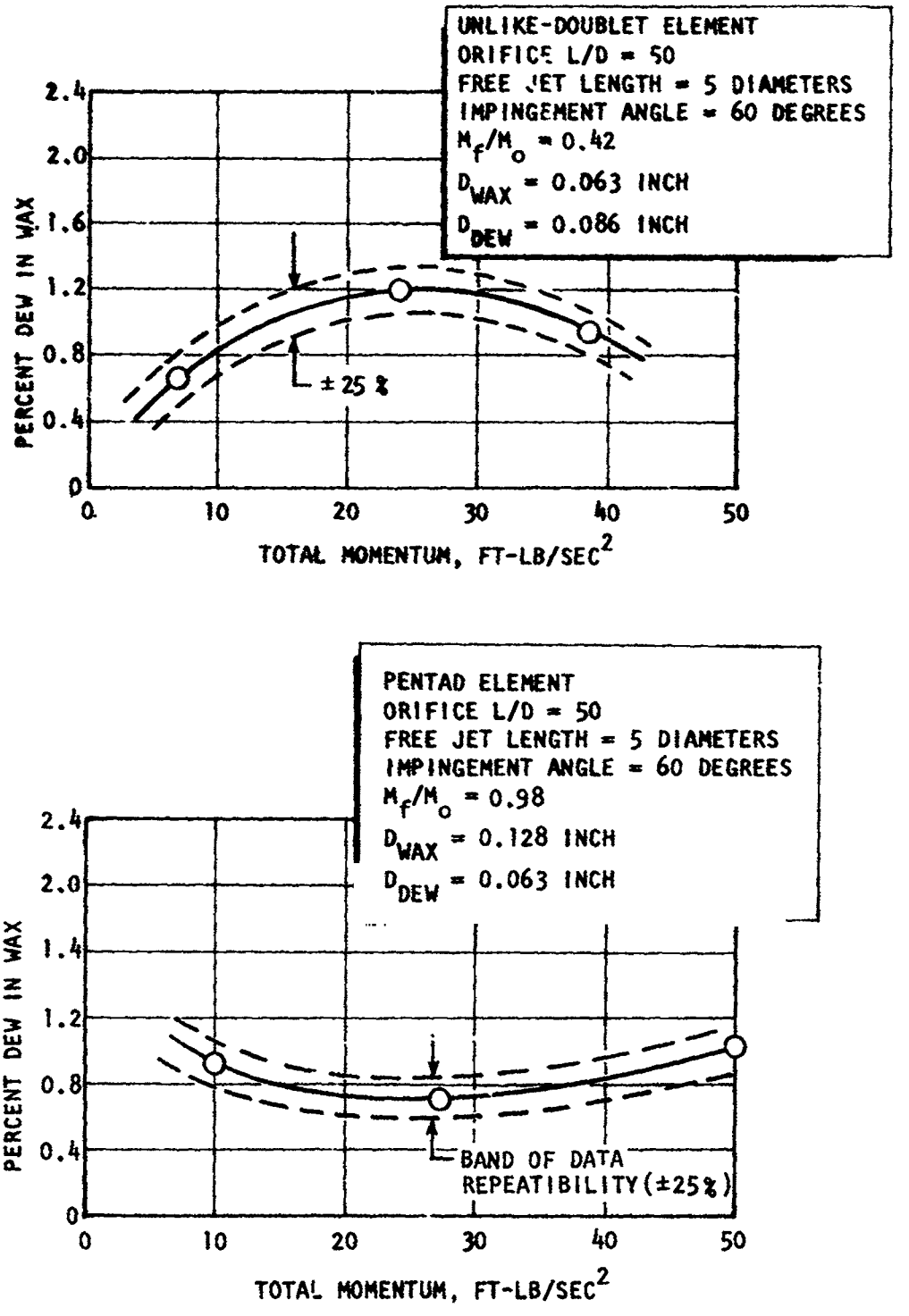

Figure 25. Percent DEW in Wax Versus Total Momentum for Unlike-Doublet and Pentad Elements

obtained at a total momentum of 20 ft-lb/sec^2 indicated a repeatibility of +25 percent from the mean. Using this error band, the amount of emulsification would appear relatively constant over the range of total momentum examined in this study.

From the results of this study, it is apparent that, even though an emulsion is formed when two immiscible liquids collide, the level of emulsification appears to be relatively invarient with momentum level for either element type. In addition, the amount of emulsification for either element appears to be similar.

TASK IIA--DROPLET SIZE DETERMINATION AT LOW INJECTION VELOCITY

An experimental investigation was conducted to determine the atomization characteristics for single element like-doublet, unlike-doublet, triplet, and pentad injectors over a range of injection velocity 30 to 60 ft/sec. This study was primarily aimed at extending the velocity range of applicability of existing empirically determined dropsize correlations (Ref. 14). The existing correlations, for all but the triplet element, were obtained over a velocity range of from 80 to 200 ft/sec. Therefore, so that all of the correlations would be applicable over the same ranges, the triplet element atomization characteristics were evaluated over a velocity range of from 30 to 171 ft/sec. The basic elements were designed with orifice L/D's of 50. In addition, for all but the triplet, experiments were conducted with elements having an orifice L/D of 10.

A summary of the element configurations and test conditions is presented in Table 8. A total of 54 experiments was made, 45 of which were conducted at the low injection velocities and an additional nine at higher velocities. For both the short L/D (10) and long L/D (50) elements, experiments were conducted at nominal injection velocities of 30, 40, (or 45), and 60 ft/sec to ascertain effects of the reduced hydraulic control present in the short L/D elements. A summary of the test data is presented in Table 9.

TABLE 8

TASK IIA ELEMENT GEOMETRY
AND TEST CONDITIONS

Element Type	D_F, inch	D_{ox}, inch	Orifice L/D	Number of Tests	Nominal Wax Injection Velocity, ft/sec
Like-Doublet	0.063	--	10	3	30, 40, 60
Like-Doublet	0.081	--		3	30, 40, 60
Unlike-Doublet	0.063	0.086		6	30, 40, 60
Unlike-Doublet	0.063	0.128		6	30, 40, 60
Pentad	0.086	0.063 (4 each)		6	30, 45, 60
Like-Doublet	0.063	--	50	3	30, 40, 60 175, 200
Unlike-Doublet	0.063	0.086		6	30, 40, 60
Pentad	0.086	0.063		6	30, 45, 60,
Triplet	0.063	0.063 (2 each)		12	30, 45, 60 90, 120, 150, 170

For all elements: Total included impingement angle = 60 degrees
Nominal free jet length = 5 diameters

TABLE 9

TASK IIA RESULTS

Run No.	Element Type	Wax System			H_2O System			Momentum Ratio, f/o	$\bar{D}$, microns
		Orifice Diameter, inch	Flowrate, lb/sec	Injection Velocity, ft/sec	Orifice Diameter, inch	Flowrate, lb/sec	Injection Velcoity, ft/sec		
1*	Like-Doublet	0.063	0.1248	60.5				--	322
2	↓	↓	0.0827	40.0				--	421
3	↓	↓	0.0622	30.1				--	465
4	↓	↓	0.0366	177.0					
5	↓	↓	0.0417	202.0					
6	Unlike-Doublet	↓	0.0616	59.7	0.086	0.0849	35.0	1.24	416
7	↓	↓	0.0417	40.4	↓	0.0749	30.9	0.73	424
8	↓	↓	0.0315	30.5	↓	0.0556	22.9	0.75	488
9	↓	0.086	0.1150	59.8	0.063	0.0814	62.6	0.74	392
10	↓	↓	0.0763	39.7	↓	0.0538	41.4	0.74	489
11	↓	↓	0.0573	29.8	↓	0.0406	31.2	0.74	521
12	Triplet	0.063 (2 each)	0.0624	30.2	↓	0.0457	35.1	0.85	583
13	↓	↓	0.0936	45.3	↓	0.0700	53.8	0.89	470
14	↓	↓	0.1243	60.2	↓	0.0943	72.5	0.91	412
15	↓	↓	0.1861	90.1	↓	0.1408	108.2	0.91	307
16	↓	↓	0.2439	118.1	↓	0.1853	142.4	0.92	266
17	↓	↓	0.3210	155.4	↓	0.2393	183.9	0.88	199
18	↓	↓	0.3540	171.0	↓	0.2583	199.0	0.85	195
19	↓	0.063	0.0315	30.5	0.063	0.0528	20.3	0.90	606
20	↓	↓	0.0465	45	(2 each)				
20	↓	↓	0.0465	45.0	↓	0.0793	30.5	0.87	484
21	↓	↓	0.0629	60.9	↓	0.1021	39.2	0.96	425
22	↓	↓	0.0935	90.5	↓	0.1542	59.3	0.93	333
23	↓	↓	0.1201	116.3	↓	0.2093	80.4	0.83	297
24	↓	↓	0.1572	152.2	↓	0.2583	99.3	0.93	238
25	Pentad	0.063 (4 each)	0.2534	61.4	0.086	0.1037	42.8	0.29	451
26	↓	↓	0.1860	45.0	↓	0.0773	31.0	0.29	503
27	↓	↓	0.1206	29.2	↓	0.0507	20.9	0.30	535

*Runs 1-30, Orifice L/D = 50
Runs 31-54, Orifice L/D = 10

TABLE 9

(Concluded)

Run No.	Element Type	Wax System			H_2O System			Momentum Ratio, f/o	$\overline{D}$, microns
		Orifice Diameter, inch	Flowrate, lb/sec	Injection Velocity ft/sec	Orifice Diameter, inch	Flowrate, lb/sec	Injection Velocity, ft/sec		
28	Pentad	0.086	0.1156	60.1	0.063 (4 each)	0.3659	70.3	0.27	292
29	↓	↓	0.0860	44.7	↓	0.2623	50.4	0.29	432
30	↓	↓	0.0583	30.3	↓	0.1815	34.9	0.28	488
31*	Like-Doublet	0.063	0.0620	30.0	↓	↓	↓	--	463
32	↓	↓	0.0834	40.4	↓	↓	↓	--	423
33	↓	↓	0.1236	59.8	↓	↓	↓	--	387
34	↓	0.081	0.1016	29.8	↓	↓	↓	--	505
35	↓	↓	0.1313	38.5	↓	↓	↓	--	493
36	↓	↓	0.1992	58.4	↓	↓	↓	--	438
37	Unlike-Doublet	0.063	0.0316	30.6	0.086	0.0554	22.9	0.76	585
38	↓	↓	0.0413	40.0	↓	0.0747	30.8	0.72	560
39	↓	↓	0.0620	60.0	↓	0.0867	35.8	1.20	474
40	↓	0.080	0.0575	29.9	0.063	0.0404	31.1	0.73	597
41	↓	↓	0.0771	40.1	↓	0.0542	41.7	0.73	568
42	↓	↓	0.1158	60.2	↓	0.0818	62.9	0.74	495
43	Unlike-Doublet	0.063	0.0316	30.6	0.128	0.0990	18.4	0.53	587
44	↓	↓	0.0411	39.8	↓	0.1335	24.9	0.49	591
45	↓	↓	0.0624	60.4	↓	0.2128	39.6	0.45	526
46	↓	0.128	0.1328	31.2	0.086	0.0493	37.9	0.45	596
47	↓	↓	0.1713	40.2	↓	0.0665	51.1	0.49	584
48	↓	↓	0.2534	59.4	↓	0.1005	77.2	0.51	455
49	Pentad	0.063 (4 each)	0.1211	29.6	↓	0.0526	21.7	0.32	517
50	↓	↓	0.1880	45.5	↓	0.0780	32.2	0.29	522
51	↓	↓	0.2494	60.4	↓	0.1019	42.0	0.28	498
52	↓	0.086	0.0577	30.0	0.063 (4 each)	0.1780	34.2	0.28	451
53	↓	↓	0.0862	44.8	↓	0.2643	50.8	0.29	364
54	↓	↓	0.1082	56.2	↓	0.3599	69.2	0.25	299

*Runs 1-30, Orifice L/D = 50
Runs 31-54, Orifice L/D = 50

Effect of Orifice L/D on Dropsize

The atomization characteristics produced from injectors designed with orifice L/D's of 50 and 10 were studied. The 10.1 and the 50:1 L/D injectors were designed with rounded orifice entrances. The specifics of the designs are discussed in the Apparatus Section. For each of the element types (like-doublet, unlike-doublet, and unlike-pentad) and for both L/D's, experiments were conducted at a nominal 30, 40, and 60 ft/sec injection velocity with two additional tests conducted at 177 and 202 ft/sec using the 50:1 like-doublet element. The results for all the elements tested are presented in Fig. 26 in terms of the mass median dropsize as a function of injection velocity. It should be noted that the mass median dropsize for the unlike elements is presented for both the oxidizer and the fuel orifice. The individual comparisons as shown in Fig. 26 are made at identical dynamic pressure ratios, because (1) the abscissa for Fig. 26 is velocity, (2) both L/D designs for each element type had identical orifices sizes, and (3) the momentum ratio was held constant for each test with the exception of runs 4 and 36 of Table 9.

In Fig. 26a, the results of the like-doublet element study are presented. The 50 L/D element produced smaller droplets than the 10 L/D element over the range of velocities shown. This was also observed with the unlike-doublet element (Fig. 26b); however, the difference was much larger. The pentad results (Fig. 26c), however, indicated very little difference in the dropsizes produced by the two differing orifice L/D designs. A notable exception is seen for the fuel dropsize at a velocity of 45 ft/sec. There does not appear to be an obvious reason for this discrepancy.

The possible reasons for the differing dropsize produced by the 10:1 and 50:1 L/D elements are many, but the most likely would include a combination of the differing entrance conditions and orifice length, which can result in unequal velocity profiles and turbulence levels in the free jet. A further discussion of these effects is presented in the following section.

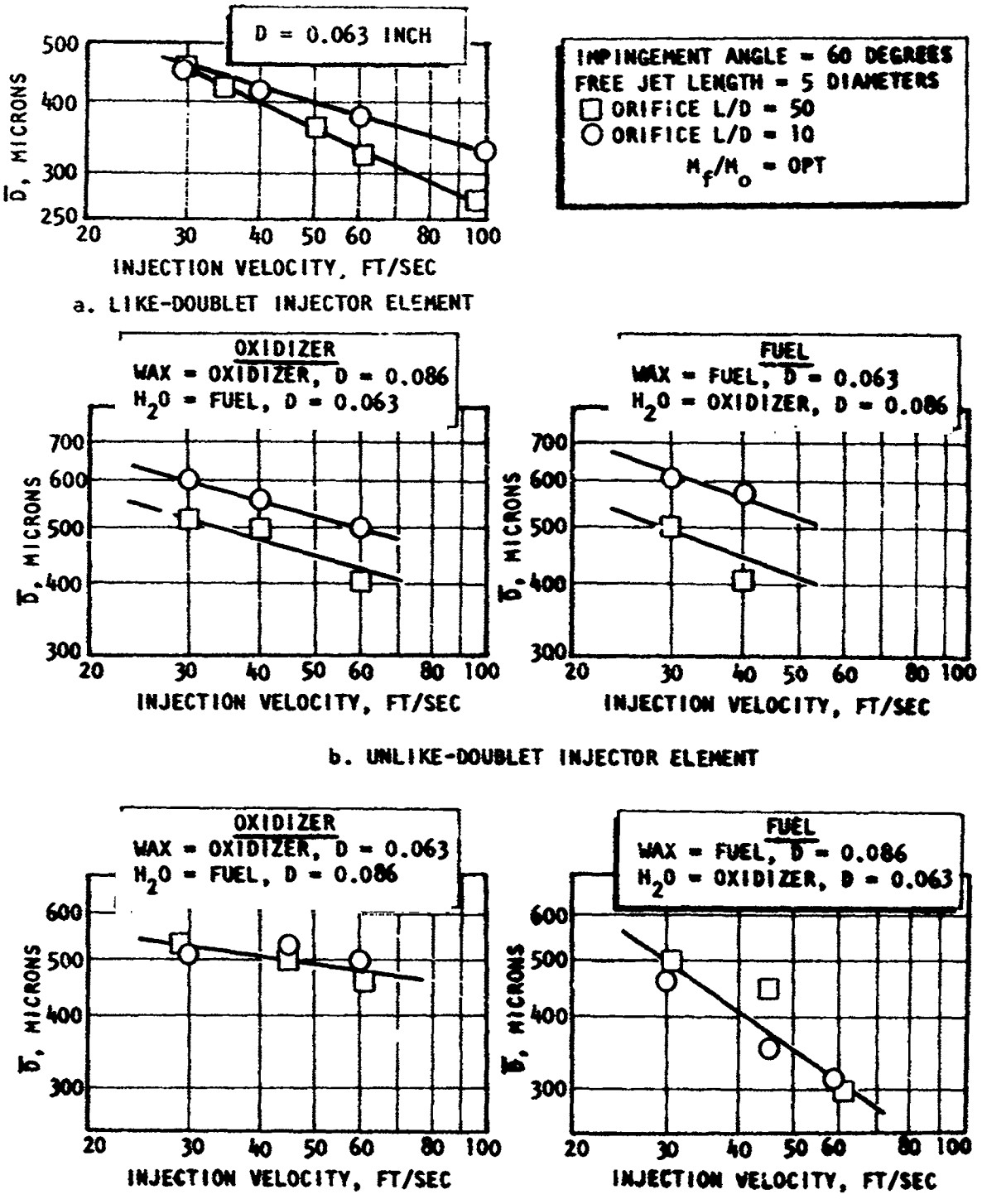

Figure 26. Comparison of Mass Median Dropsize as a Function of Injection Velocity for Two Differing Orifice L/D Designs

Like Doublet Injector Atomization

Wax flow experiments were made using three like-doublet elements: two short L/D elements having orifice diameters of 0.063 and 0.081 inch, and a long L/D element having a diameter of 0.063 inch. Three tests were conducted with each of the 10:1 L/D elements at nominal injection velocities of 30, 40, and 60 ft/sec. Five tests were made with the 50:1 element, three at the low velocities and an additional two at 175 and 205 ft/sec. The data for these three injectors are plotted in Fig. 27. Also shown in the figure are data points obtained in Task IA and from the Ref. 14 program.

In the Ref. 14 program, it was found that, over an injection velocity range of 70 to 200 ft/sec, the mass median dropsize ($\bar{D}$) could be expressed as a simple power function of the orifice diameter and velocity

$$\bar{D} = 7.84 \times 10^4 \frac{D^{0.57}}{V^{0.85}}$$

Plots of this equation for the three like-doublet elements shows excellent agreement over the range of 100 to 200 ft/sec. At velocities below this range, the dropsizes are considerably smaller than those calculated from the above equation, and at the lowest velocity investigated (30 ft/sec), the predicted dropsizes are twice as large as the experimental values.

Also shown in the figure is a plot of a modified version of the correlating equation suggested by Ingebo (Ref. 13). His data, which were obtained using n-heptane in air, gave the following relation

$$D_{30} = \frac{2.54 \times 10^4}{2.64 \sqrt{V_j/D_j} + 0.97 \, |\Delta V|}$$

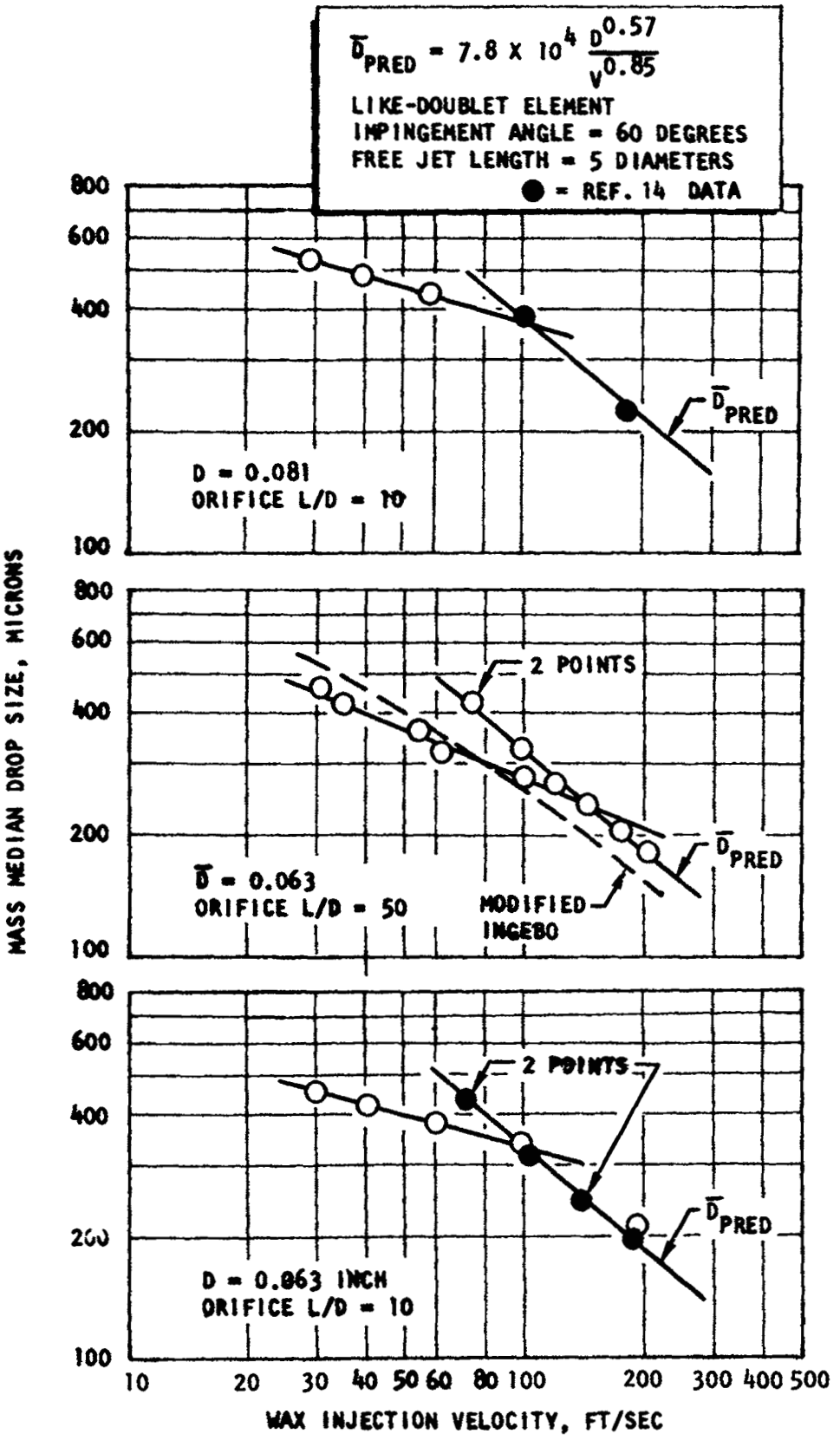

Figure 27. Mass Median Dropsize Versus Injection Velocity for Like-Doublet Injectors

where

D_{30} = volume mean droplet diameter, microns

D_j = jet diameter, microns

V_j = jet velocity, ft/sec

$|\Delta V| = |V_g - V_\ell|$ = magnitude of the gas velocity (air) minus the jet velocity, ft/sec

This equation includes terms that take into account both the primary (hydraulic) and secondary (shear) atomization processes. The term $\sqrt{V/D}$ is considered to represent primary atomization and is controlled by injector design hydraulics. The relative velocity expression ($\Delta V = V_g - V_\ell$) is considered to be the secondary atomization term and is controlled by the gas forces acting on the liquid.

To compare Ingebo's expression with the current data, a modification of his relation was necessary to account for the effects of fluid physical properties on the secondary atomization term. This was accomplished as follows.

Other work by Ingebo (Ref. 17) indicated that the effects of liquid viscosity, density, and surface tension could be accounted by

$$K = \left[\left(\frac{\mu_L \sigma_L}{\rho_L} \right)_{\text{n-heptane}} \Big/ \left(\frac{\mu_L \sigma_L}{\rho_L} \right)_{\text{wax}} \right]^{1/4}$$

where

ρ = density

μ = viscosity

σ = surface tension

In addition, it was necessary to convert from volume mean dropsize (D_{30}) to mass median dropsize ($\bar{D}$). Dickerson (Ref. 14) found that for like-doublet injectors the conversion factor was

$$\bar{D} = 1.52\, D_{30} \quad \text{(assuming constant distribution)}$$

The resulting expression for calculating the wax dropsize is:

$$\bar{D} = \frac{38{,}720}{2.64\sqrt{V_j/D_j} + 0.97K\,|\Delta V|}$$

where

K = property correction factor = 0.56

ΔV = V_j (V_g = 0 during this study)

A plot of this expression in Fig. 27 shows reasonable agreement with the experimental data. However, inspection of the data presented in Fig. 27 suggests the existence of two distinct atomization regimes with a transition region (in which the data scatter was significantly greater than usual) in the velocity range of approximately 70 to 130 ft/sec. This trend is not suggested from the results of Ingebo.

A comparison of the dropsizes produced by the 10:1 and 50:1 elements reveals two slight variations in the trend of the data. First, at the lowest injection velocity of 30 ft/sec the two orifices produce almost identical dropsizes. However, as the velocity increases, the droplet sizes produced by the 50:1 L/D element are smaller than those of the corresponding 10:1 L/D element. (It should be noted that the difference is small; however, the trend is consistent.) Second, the transition point with the 10:1 orifice occurs at about 100 ft/sec whereas that for the 50:1 orifice appears occur to at a higher velocity (about 140 ft/sec).

Examination of the orifice and inlet geometry for the two elements suggests some possible explanations for these apparent anomalies. For the long orifices, the upstream flow section had a cross section of five orifice diameters versus three orifice diameters for the short orifices. The entry lengths for both configurations were both 50 orifice diameters in length. Calculation of the Reynolds number of the entrance shows that, for both elements, the break in the shape of the dropsize-velocity curve occurs in the range of 3000 to 4000. This suggests that the change in the atomization characteristics might be attributed to a transition from laminar to turbulent entry flow. The slight variations in dropsize at the low injection velocities could possibly be due to the fact that the long orifice has sufficient length to enable nearly complete development of turbulent flow at the orifice exit. This is not the case for the short (10:1 L/D) orifice. An approximate analysis (assuming one-dimensional flow and a quiescent inlet) indicated that at a length of 10 diameters, the boundary layer growth was only 25 percent completed.

There are other possible explanations for the break in the dropsize-velocity curves. First, the generation of large dropsizes at low injection velocities may be limited by the relative aerodynamic effects between the droplets and the surrounding gas which can cause secondary droplet shattering to occur. In addition, the sheet produced by the impingement of the jets may disintegrate because of hydrodynamic instability in the low velocity regime with aerodynamic interactions controlling breakup at the higher velocities. While all of the above appear possible, sufficient data are not available to ascertain which mechanism (or combination of) is controlling.

Unlike-Doublet Injector Atomization

Molten wax experiments were conducted with three unlike-doublet injection elements at nominal injection velocities of 30, 40, and 60 ft/sec. Two of these elements incorporated a 10:1 orifice L/D and diameter ratios of 1.36 and 2.03 (d_{oxid}/d_{fuel}). The 50:1 L/D element had a diameter ratio of 1.36. In all cases, the fuel orifice diameter (the smaller of the two)

was 0.063 inch. In addition, all tests were conducted at the condition which produces optimum propellant mixing. The dropsize data for the two diameter ratios are presented in Fig. 28 and 29. A comparison of the unlike-doublet data with that for the like-doublet shows that, at low injection velocities, the dropsizes are considerably smaller than predicted from the equations of Ref. 14. This is the same trend observed with the like-doublet elements.

A comparison of the fuel and oxidizer dropsizes (where $d_f < d_o$) shows that the oxidizer droplet sizes are generally larger than those for the fuel. This is as expected since, for the two cases shown, the oxidizer orifice diameter is the larger of the two. It is significant to note, however, that as injection velocity approaches 30 ft/sec, the two appear to approach a maximum dropsize of 600 microns.

Pentad (4-on-1) Injector Atomization

Experiments were conducted with two pentad elements at nominal injection velocities of 30, 45, and 60 ft/sec. Both short (10:1) and long (50:1) elements were used. Other than orifice L/D, the two elements were similar, with a central (fuel) orifice of 0.086 inch diameter, and four outer (oxidizer) orifices 0.063 inch.

The results for the pentad elements are presented in Fig. 30. The tendency for the dropsizes to be smaller than predicted (by the relations given in Ref. 14) is again in evidence at injection velocities below about 100 ft/sec.

Triplet (2-on-1) Injector Atomization

A series of 13 tests was conducted with a 50:1 L/D coplaner triplet element (i.e., two outer jets impinging on a central jet). The experiments were conducted over a range of injection velcoties from 30 to 171 ft/sec. This range was investigated because no data were known to exist for this type of element configuration. The orifice diameter ratio for these tests was constant at 1.0 ($d_f = d_{ox} = 0.063$ inch).

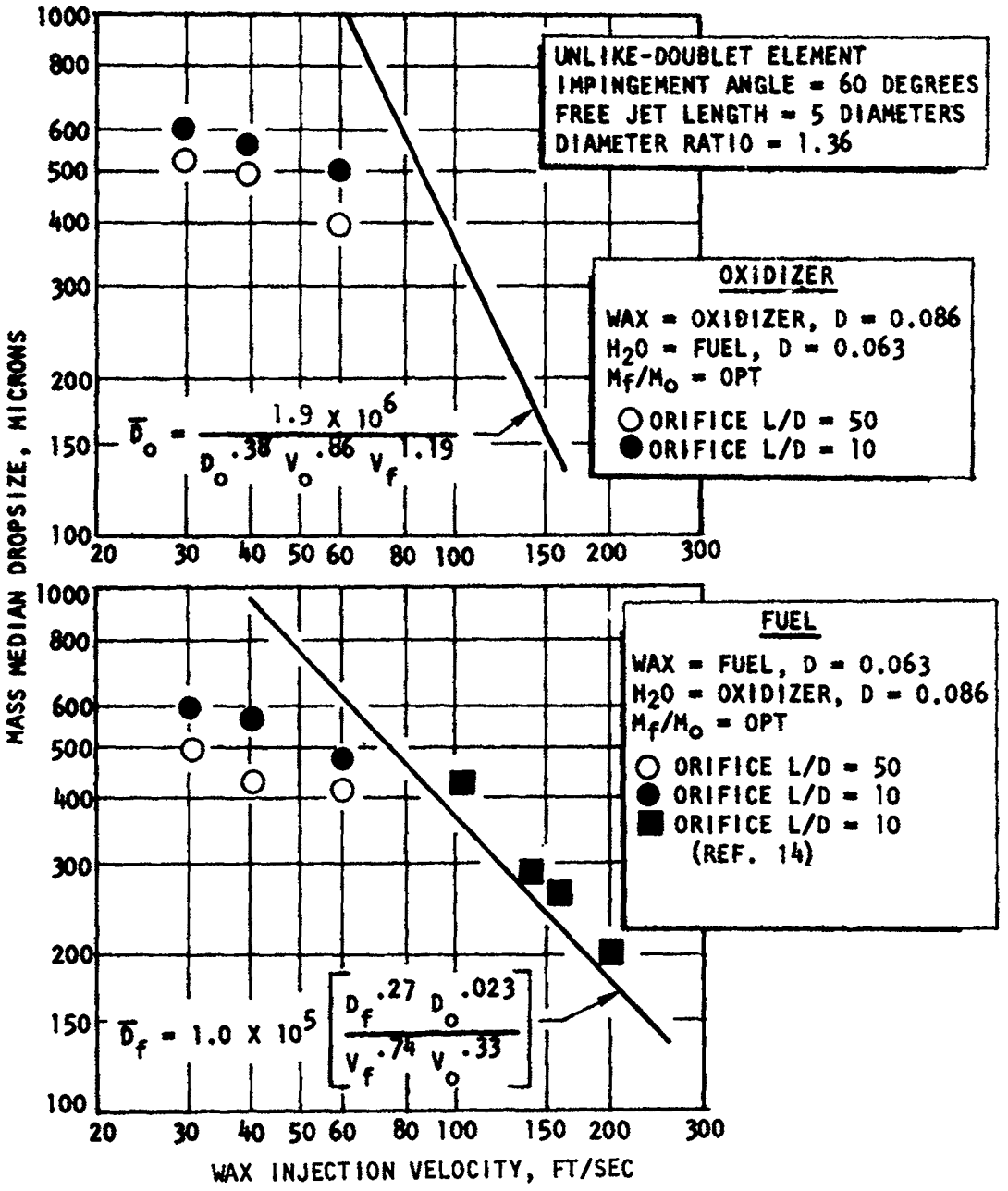

Figure 28. Mass Median Dropsize Versus Injection Velocity for an Unlike-Doublet Element Having a Diameter Ratio of 1.36

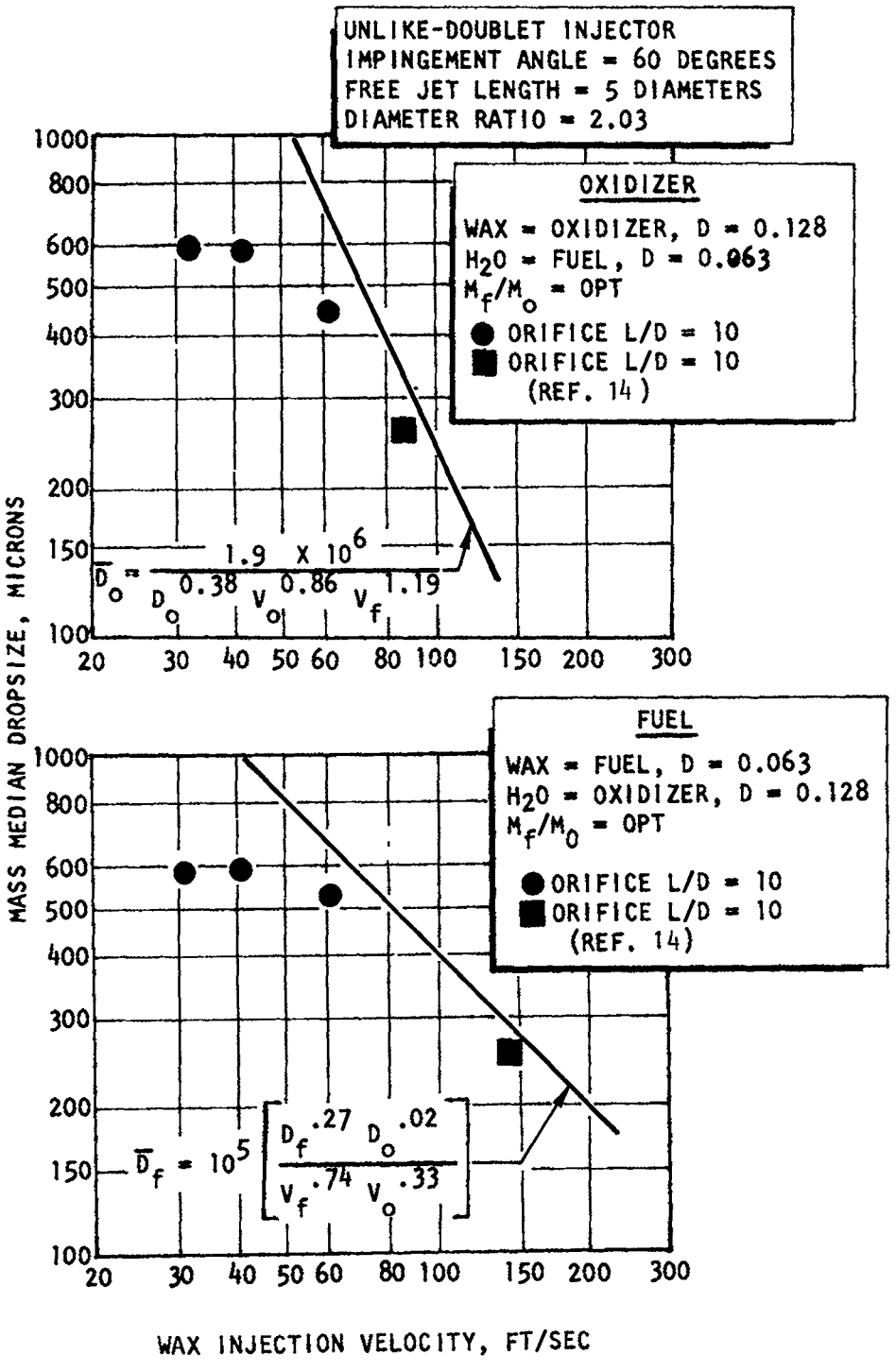

Figure 29. Mass Median Dropsize Versus Injection Velocity for an Unlike-Doublet Injector Having a Diameter Ratio of 2.03

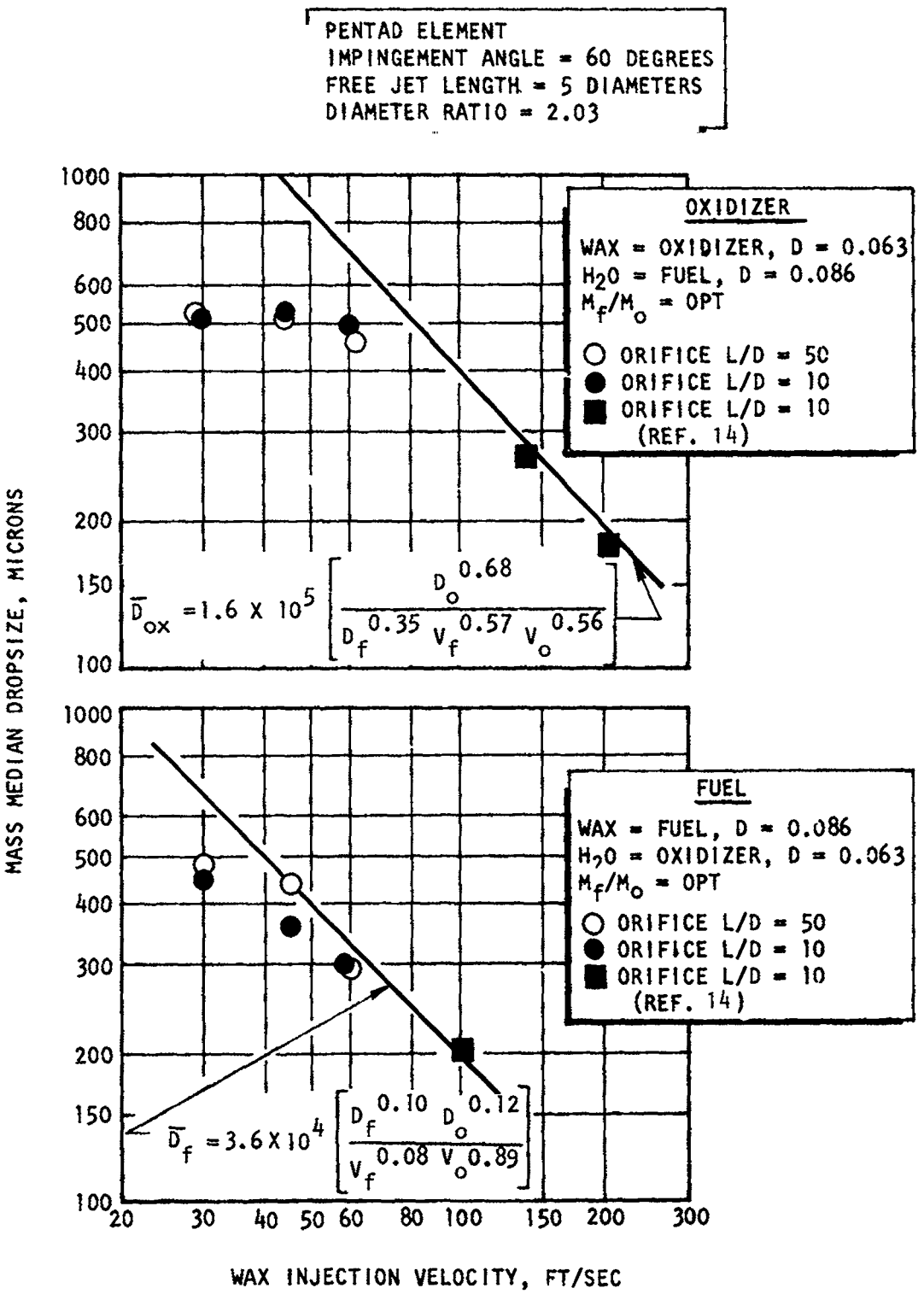

Figure 30. Mass Median Dropsize Versus Injection Velocity for a Pentad Element

Dropsize data for the triplet element are presented in Fig. 31. The data shows that almost identical dropsize versus velocity relationships were obtained for both fuel (wax flowed through the central orifice) and oxidizer (wax flowed through the outer two orifices). This may be attributed to the fact that the two orifice diameters were equal, and the injection velocities (computed on the basis of optimum mixing) are nearly equal.

Examination of Fig. 31 shows that the triplet element produced a linear dropsize-velocity relationship over the majority of the velocity regime investigated. A break in the curve is suggested; however, the exact point is not as well defined as those of the other element types. The shape of the data at high velocity (Fig. 31) represents an estimated value based on the pentad results.

TASK IIB--FREE JET EFFECTS

For most injector element types, the impingement angle and free jet length may affect both face splashing and propellant atomization. Face splashing can be a serious problem resulting in injector face burnout. Long free jet lengths result in the impingement of streams that may be already partially disintegrated. The objective of this task was to quantitatively determine the effect of impingement angle and free jet length on spray dropsize.

A total of 28 wax flows were conducted to fulfill the task objectives. All tests were made with the 50 orifice L/D like doublet element having a constant orifice diameter of 0.063 inches. Measurements of dropsize were made at impingement angles of 45, 60, and 90 degrees, free jet lengths of 1, 5, and 10 diameters, and mean injection velocities of 70, 95, and 120 ft/sec. The data are presented in Table 10.

The effect of free jet length on mass median dropsize is shown in Fig. 32. (The data at 70 ft/sec were not included because of the large amount of data scatter encountered at this velocity level in the Task IIA experiments).

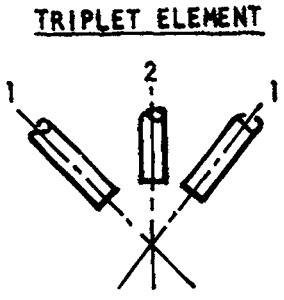

ORIFICE L/D = 50
FREE JET LENGTH = 5 DIAMETERS
IMPINGEMENT ANGLE = 60 DEGREES
$D_1 = D_2 = 0.063$ INCH

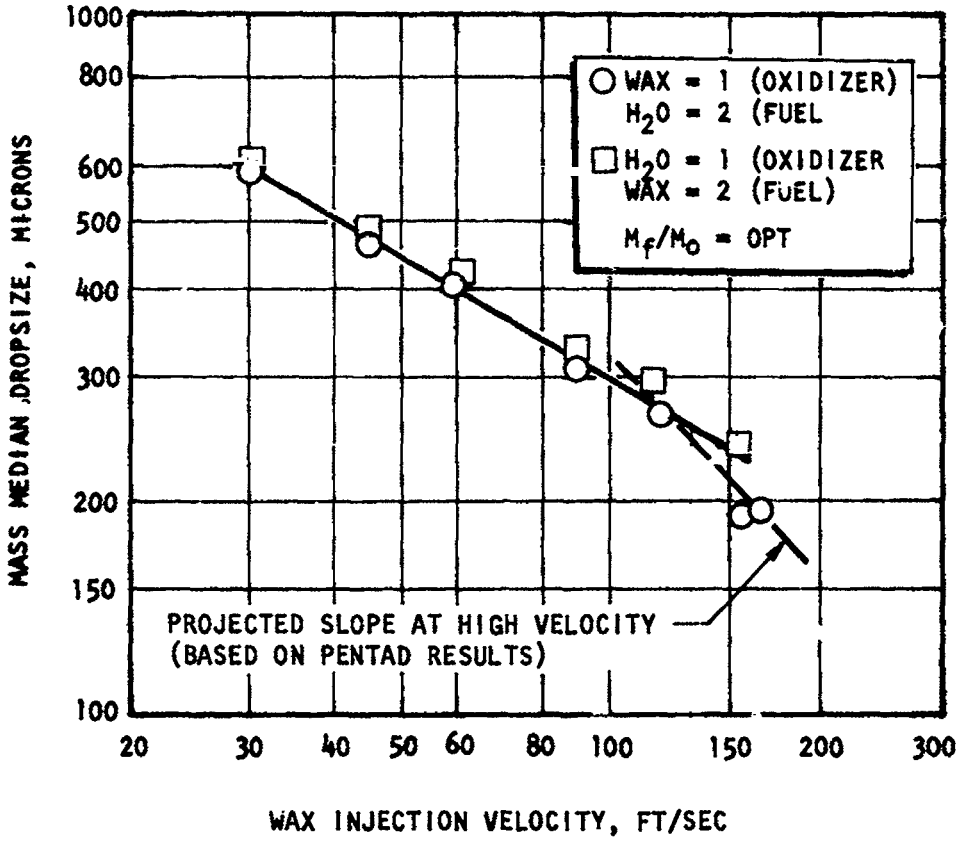

Figure 31. Mass Median Dropsize Versus Injection Velocity for a Triplet Element

TABLE 10

TASK IIB WAX FLOW RESULTS, LIKE-DOUBLET ELEMENT,
ORIFICE L/D = 50, ORIFICE DIAMETER = 0.063 INCH

Run No.	Impingement Angle, degrees	Free Stream, L/D	Flowrate, lb/sec	Injection Velocity, ft/sec	$\bar{D}$, microns
1	60	5	0.0764	73.7	422
2	↓	↓	0.1000	96.5	325
3	↓	↓	0.1225	118.2	268
4	↓	1	0.0715	69.0	370
5	↓	↓	0.0990	95.5	295
6	↓	↓	0.1274	123.0	250
7	↓	10	0.1220	117.7	317
8	↓	↓	0.1019	98.3	383
9	↓	↓	0.0725	70.0	400
10	45	1	0.1245	120.2	265
11	↓	↓	0.1009	97.4	275
12	↓	↓	0.0657	63.4	440
13	↓	5	0.1225	118.2	290
14	↓	↓	0.0981	94.7	320
15	↓	↓	0.0715	69.0	430
16	↓	10	0.1230	118.7	340
17	↓	↓	0.0970	93.6	420
18	↓	↓	0.0706	68.1	495
19	90	1	0.1215	117.3	195
20	↓	↓	0.1245	120.2	195
21	↓	↓	0.1021	98.5	197
22	↓	↓	0.0686	66.2	306
23	↓	5	0.1213	117.1	210
24	↓	↓	0.1008	97.3	205
25	↓	↓	0.0708	68.3	282
26	↓	10	0.1254	121.0	278
27	↓	↓	0.0988	95.4	272
28	↓	↓	0.0715	69.0	270

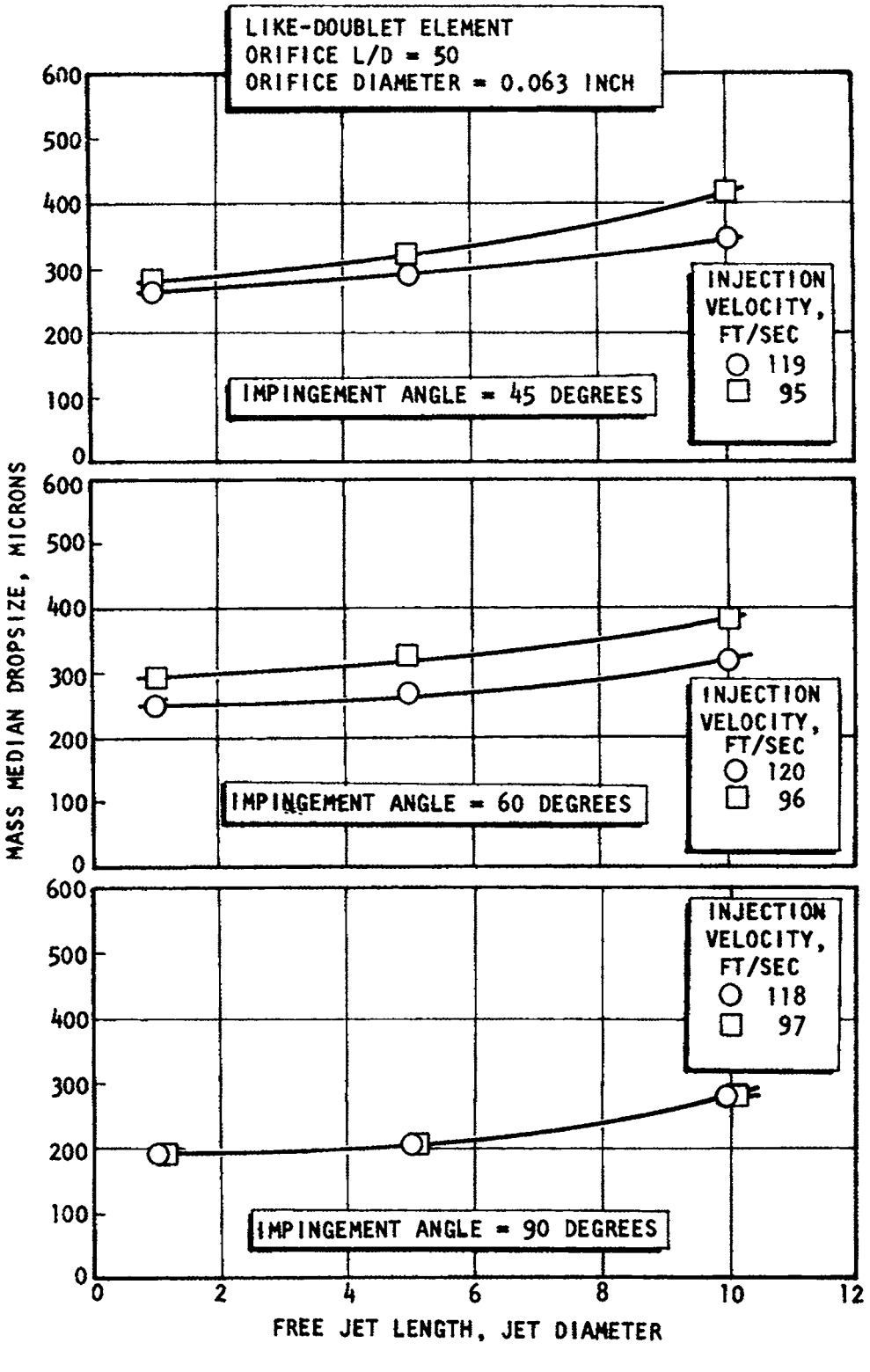

Figure 32. Mass Median Dropsize Versus Free Jet Length for Like-Doublet Elements

Examination of this figure shows that the general trend was for drop size to increase with a corresponding increase of free jet length. The largest percentage increase (≈40) was observed at the 90-degree impingement angle and nominal injection velocities of 97 and 113 ft/sec. This would indicate that as the velocity of the two impinging jets is increased, the efficiency of momentum exchange is critically dependent upon such factors as jet alignment, free jet breakup, etc.

The causes for the increase of dropsize at the longer free jet lengths are postulated as being caused by increasing jet breakup, decreasing jet turbulence, and possible jet misalignment. Extreme care was exercised to ensure that misimpingement did not occur. Measurement of orifice tube position indicated centerline alignment within 0.002 inches.

The effect of impingement angle on dropsize is shown in Fig. 33. In addition to the experimental data from this program, the correlating equations of Dombrowski and Hooper (Ref. 12) and Fry, Thomas, and Smart (Ref. 18) relating dropsize to impingement angle are included for reference. It is interesting to note the wide discrepancy in the two correlations, particularly at the impingement angle of 45 degrees. Although both investigators used a photographic technique to measure particle sizes, Dombrowski and Hooper investigated only the central portion of the spray field. From spray photographs of Ref. 12, it appears that at small impingement angles, the mass flux and droplet sizes are both high in the central portion of the spray. This is in contrast to the larger impingement angles in which the mass flux and dropsize appear more uniformly dispersed. This would then account for the extremely large droplet sizes reported by Dombrowski and Hooper at the lower impingement angles.

Examination of Fig. 33 shows good agreement of the current data with the correlation of Fry, et al. The wax flow results were found to agree within ±10 percent for impingement angles of 45 to 90 degrees.

A comparison of the like-doublet dropsize distribution produced at various free jet lengths is shown in Fig. 34. No major variations in the distribution curves were observed at the impingement angles of 45, 60, and 90 degrees. The same conclusion can be drawn from Fig. 35 which illustrates the distributions obtained at the three impingement angles.

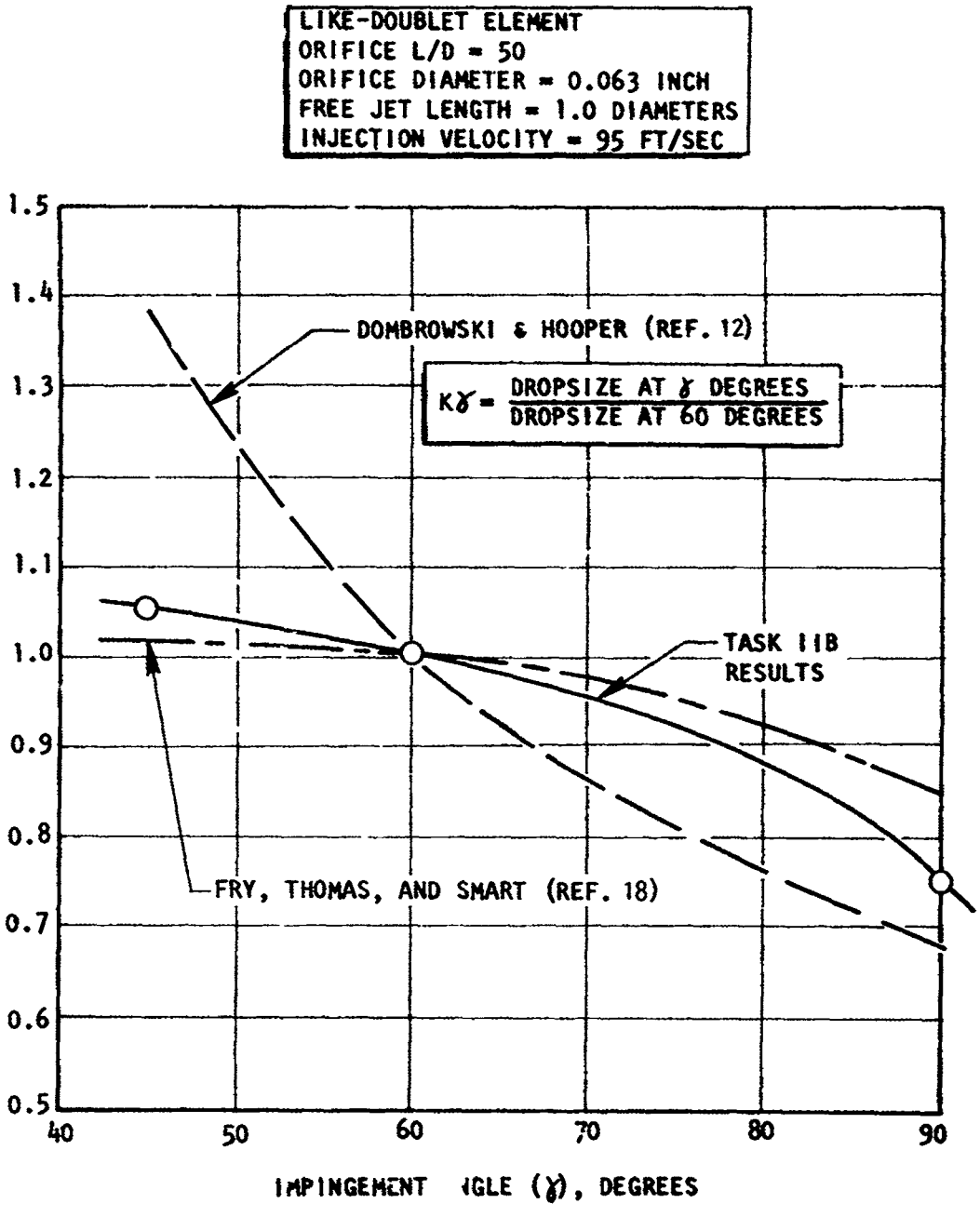

Figure 33. Drop Size Ratio Versus Impingement Angle for Like-Doublet Element

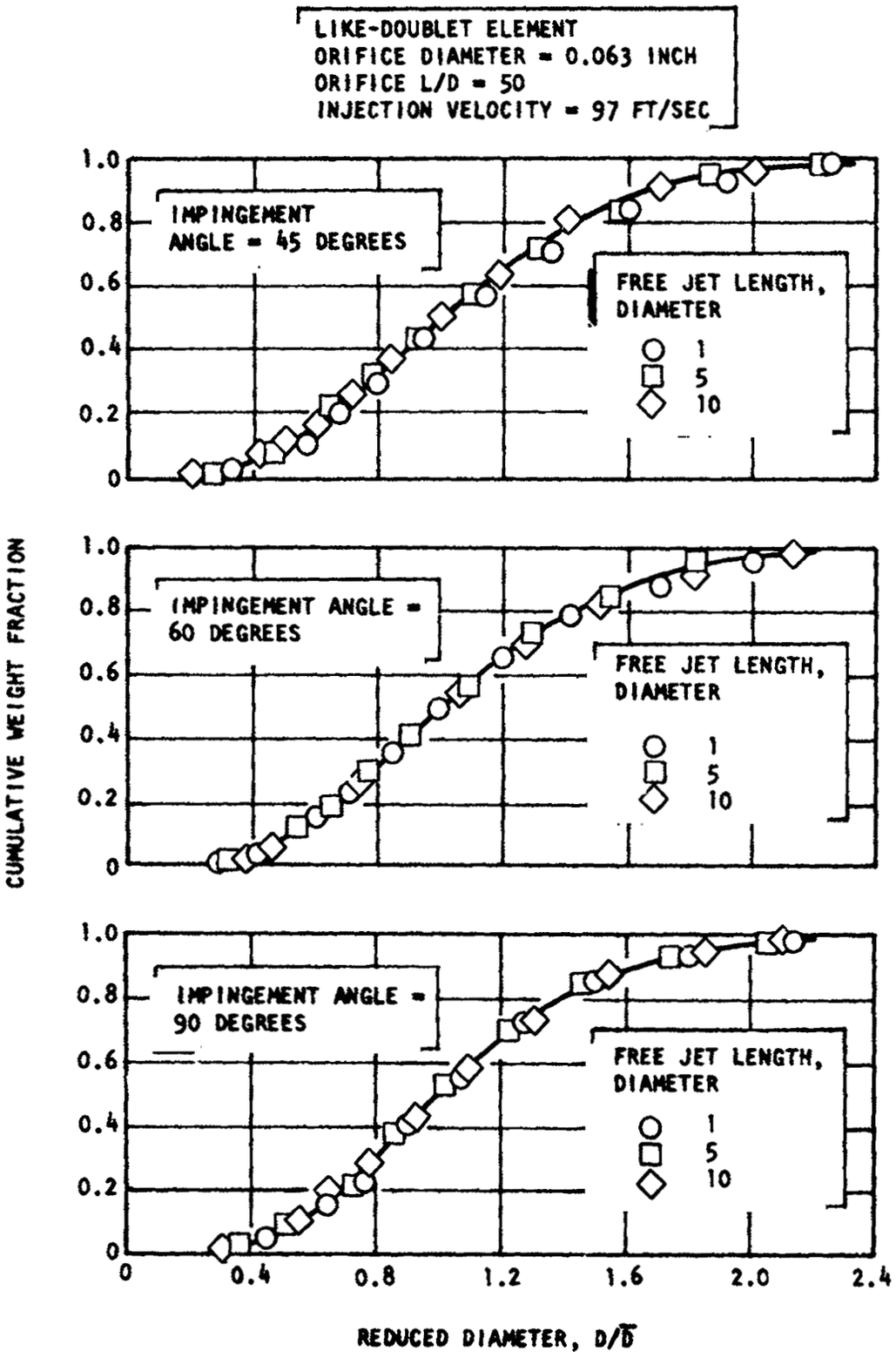

Figure 34. Normalized Distribution Curves for Unlike-Doublet Elements at Various Free Jet Lengths

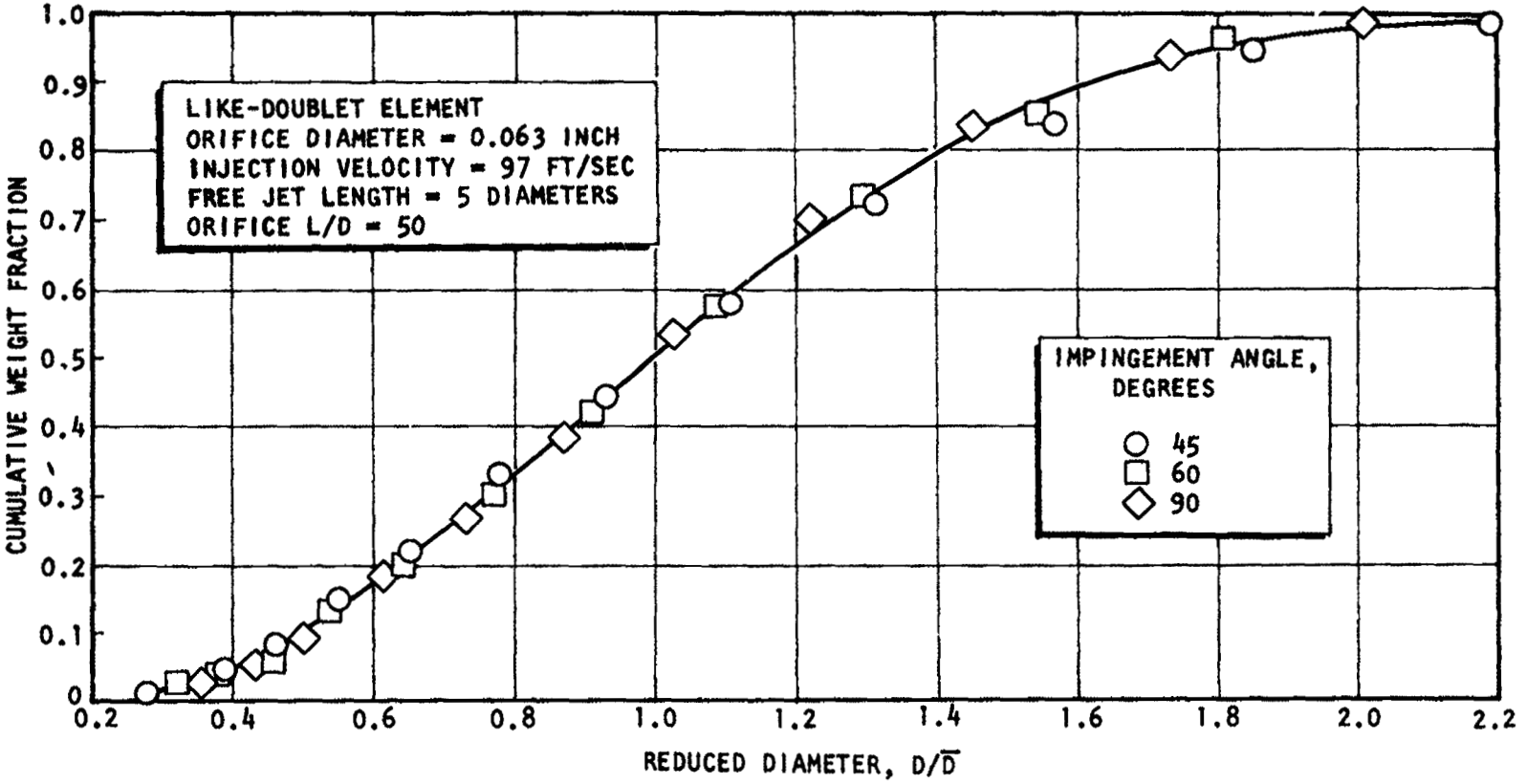

Figure 35. Normalized Distribution Curve for Like Doublet Element at Various Impingement Angles

CONCLUSIONS AND RECOMMENDATIONS

The major conclusions that can be made as a result of this study are: (1) the molten wax technique is an ideal experimental tool for studying the mechanisms governing atomization, and (2) the ability to predict dropsize for impinging stream injectors requires analytical knowledge of the influence of more injector mechanical and hydraulic parameters than those specified in available correlations. The molten wax technique is a useful experimental tool for studying the atomization process for several reasons. First, the entire spray field is readily analyzed, and consequently the dropsize and size distribution results are therefore not influenced by such factors as depth of field and measurement location which are encountered with photographic techniques. Secondly, through the use of immiscible liquids, the wax technique permits the direct measurement of both fuel and oxidizer sprays resulting from unlike impinging injector elements. Finally, this technique is economical primarily because of the simple sieve analysis used to determine the spray size distribution.

Previous investigations of the atomization characteristics of impinging stream injectors have generally been limited to a study of the effects of orifice diameter, injection velocity, and impingement angle on dropsize and size distribution. The results of this study have shown that additional variables, such as orifice geometry, free jet geometry, and dynamic pressure ratio, can also be critically important.

In addition, an unanticipated break in the dropsize-velocity curves was observed for all of the injector types investigated. The reasons for this occurrence were not evident; however, it was postulated that changes in the upstream flow conditions and/or the mechanisms of sheet disintegration were primarily responsible for this phenomenon.

Recommendations for future work resulting from observations in this study are as follows:

1. Injector design variables and operating conditions have been observed to influence spray dropsize and distribution. The most significant of these were the orifice diameter ratio and the dynamic pressure ratio. Both miscible and immiscible experiments are suggested to independently determine the influence of these variables.

2. It has been postulated that operation at equal dynamic pressures (as in like doublets) results in unstable droplet breakup. Experiments with doublet injectors are suggested to determine if any discontinuous processes occur at this condition.

3. The reasons for the change in the dropsize-velocity dependence should be thoroughly investigated. Specific areas of study recommended include orifice and entrance geometry and flow conditions, secondary atomization, and the mechanisms of sheet disintegration.

4. The effects of jet turbulence and velocity profile, jet disintegration, and misimpingement on dropsize are essentially unknown. A study of this type should include not only long L/D orifices which yield controlled hydraulic characteristics, but also the short, sharp edge orifices which are found in many operational injectors.

REFERENCES

1. Lord Rayleigh (J. W. Strutt), "On the Instability of Jets," Proc. of London Math Soc., V10, 1878, p. 4.

2. Lord Rayleigh (J. W. Strutt), On the Stability of a Cylinder of Viscous Liquid Under Capillary Force, Phil. Mag., V37, 1892, p. 153.

3. Weber, C., "On the Breakdown of a Fluid Jet," Ninth Progress Report, V11, 1931, Project MX-833, Sect. II, University of Colorado, Boulder, Colorado.

4. Baron, T., Atomization of Liquid Jets and Droplets; University of Illinois Technical Report No. 4, February 15, 1949.

5. Borodin, V. A., and Dityakin, Unstable Capillary Waves on the Surface of Separation of Two Viscous Liquids, NACA Tech. Memo No. 1281, April 1951.

6. Balje, O. E., and Larson, The Mechanism of Jet Disintegration, AAF Air Material Command, Engineering Division Memorandum Report No. MCREXE-664-531B; GS-USAF-Wright Patterson No. 179, August 1949.

7. Heidmann, M. F., R. Priem, and J. Humphrey, A Study of Sprays Formed by Two Impinging Jets, NACA TN 3835, March 1957.

8. Dombrowski, N. and R. Fraser, A Photographic Investigation Into the Disintegration of Liquid Sheets, British Chemical Engineering, V247, A-924, September 1954, p. 101.

9. Hagerty, W. W. and J. Shea, A Study of the Stability of Plane Fluid Sheets, Journal of Applied Mechanics, December 1955, p. 510.

10. Tanasawa, Y., The Atomization of Liquid by Means of Flat Impingement, Preprint No. 356-56, American Rocket Society, 1956.

11. Schweitzer, P. H., Factors in Diesel Spray Nozzle Design in the Light of Recent Oil-Spray Research, ASME Transactions, V52, 1930, p. 121.

12. Dombrowski, N. and P. Hooper, A Study of the Sprays Formed by Impinging Jets in Laminar and Turbulent Flow, Journal of Fluid Mechanics, V18, Part 3, pp. 392-400, 1964.

13. Ingebo, R. D., Dropsize Distributions for Impinging-Jet Breakup in Airstreams Simulating the Velocity Conditions in Rocket Combustors, NACA TN 4222, March 1958.

14. AFRPL-TR-68-147, Correlation of Spray Injector Parameters With Rocket Engine Performance, Final Technical Report, Rocketdyne, a division of North American Rockwell Corporation, Canoga Park, California, June 1968.

15. Rupe, J. H., On the Dynamic Characteristics of Free-Liquid Jets and a Partial Correlation With Orifice Geometry, TR 32-207, Jet Propulsion Laboratory, Pasadena, California, January 1962.

16. Rupe, J. H., A Correlation Between the Dynamic Properties of a Pair of Impinging Streams and the Uniformity of Mixture-Ratio Distribution in the Resulting Spray, Progress Report No. 20-209, Jet Propulsion Laboratory, Pasadena, California, 28 March 1956.

17. Ingebo, R. D., et al., Dropsize Distribution for Crosscurrent Breakup of Liquid Jets in Airstreams, NACA TN 4087, 1957.

18. Fry, F., P. Thomas, and P. Smart, Institute of Fire Engineers, Edinborough, England, 1954.